(2)



214700-1-F

Final Report

# EO TARGET ENHANCEMENT DEMONSTRATION



C.T. DUE
W.L. CESAROTTI

DECEMBER 1989

Unlimited distribution

Sponsored by:
U.S. Army Corps of Engineers
U.S. Army LABCOM
2800 Power Mill Rd.
Adelphi, MD 20783-1197

Monitored by:
U.S. Army Engineers
Waterways Experiment Station
Vicksburg, MS 39180-0631





# REPORT DOCUMENTATION PAGE

Form Approved OMB No. 0704-0188

| | |
|---|---|
| 1a. REPORT SECURITY CLASSIFICATION: Unclassified | 1b. RESTRICTIVE MARKINGS |
| 2a. SECURITY CLASSIFICATION AUTHORITY | 3. DISTRIBUTION/AVAILABILITY OF REPORT: Unlimited |
| 2b. DECLASSIFICATION/DOWNGRADING SCHEDULE | |
| 4. PERFORMING ORGANIZATION REPORT NUMBERS(S): 214700-1-F | 5. MONITORING ORGANIZATION REPORT NUMBER(S) |
| 6a. NAME OF PERFORMING ORGANIZATION: ERIM; 6b. OFFICE SYMBOL (If applicable) | 7a. NAME OF MONITORING ORGANIZATION: USAE Waterways Experiment Station (WESEN-B) |
| 6c. ADDRESS (City, State, and ZIP Code): P. O. Box 8618, Ann Arbor, MI 48107 | 7b. ADDRESS (City, State, and ZIP Code): P. O. Box 631, Vicksburg, MS 39181-0631 |
| 8a. NAME OF FUNDING /SPONSORING ORGANIZATION: US Army LABCOM/ US Army Corps of Engineers; 8b. OFFICE SYMBOL (If applicable): AMSLC-TP | 9. PROCUREMENT INSTRUMENT IDENTIFICATION NUMBER: DACA39-89-K-0005 |
| 8c. ADDRESS (City, State, and ZIP Code): 2800 Powder Mill Road, Adelphi, MD 20783-1197 | 10. SOURCE OF FUNDING NUMBERS: PROGRAM ELEMENT NO. / PROJECT NO / TASK NO. / WORK UNIT ACCESSION NO. |

11. TITLE (Include Security Classification): EO Target Enhancement Demonstration

12. PERSONAL AUTHOR(S): C. T. Due, W. L. Cesarotti

| 13a. TYPE OF REPORT | 13b. TIME COVERED | 14. DATE OF REPORT (Year, Month, Day) | 15. PAGE COUNT |
|---|---|---|---|
| Final | FROM Dec 88 TO Dec 89 | 1989 December | 184 |

16. SUPPLEMENTARY NOTATION

| 17. COSATI CODES | | | 18. SUBJECT TERMS (Continue on reverse if necessary and identify by block number) |
|---|---|---|---|
| FIELD | GROUP | SUB-GROUP | |
| | | | |
| | | | |

19. ABSTRACT (Continue on reverse if necessary and identify by block number)

This program investigated potential improvements in the detection capability of direct-view, electro-optical viewers through the use of unexploited polarization and spectral signatures. The focus of the demonstration was on low cost improvements to inventory devices. The improvement technique pursued was the overlay of the target signature on the scene being viewed. The viewing devices used were a third generation Low Light Level ($L^3$) viewer and a CCD camera. Demonstration testing was conducted at two sites at the Waterways Experiment Station for a variety of target and scenario conditions. Test data were analyzed qualitatively and quantitatively. The quantitative analysis provided the analytical foundation for the program conclusions and recommendation. The investigators concluded that while polarization signatures were observed, the signature contrast was limited by the noise of the $L^3$ viewer and judged to have little utility in enhancing target detection (cont'd)

| 20. DISTRIBUTION/AVAILABILITY OF ABSTRACT | 21. ABSTRACT SECURITY CLASSIFICATION |
|---|---|
| ☒ UNCLASSIFIED/UNLIMITED ☐ SAME AS RPT ☐ DTIC USERS | Unclassified |

| 22a. NAME OF RESPONSIBLE INDIVIDUAL | 22b. TELEPHONE (Include Area Code) | 22c. OFFICE SYMBOL |
|---|---|---|
| | | |

19. ABSTRACT (continued)

capability of these instruments. The qualitative analysis and image statistics for the spectral signature portion of the demonstration suggested the technique of spectral filtering may significantly enhance target detection, and further examination of this phenomenology is recommended.

TABLE OF CONTENTS

## LIST OF FIGURES

LIST OF FIGURES (continued)

LIST OF TABLES

# EXECUTIVE SUMMARY

## BACKGROUND AND OBJECTIVE

The EO Target Enhancement Demonstration program, conducted under USAE Waterways Experiment Station contract DACA39-89-K-0005, was initiated as an Environmental Research Institute of Michigan (ERIM) proposed program under Area 1 [Reconnaissance, Surveillance, and Target Acquisition (RSTA)] of the U.S. Army LABCOM Broad Agency Announcement (BAA) dated January 1988. The objectives of the program were to investigate and demonstrate potential improvements in the RSTA capabilities of conventional, ground-to-ground, man-in-the-loop, electro-optical systems, using the noted unexploited signatures of targets. To minimize the cost of the study, the demonstration hardware was constrained to include only minor modifications to existing, fielded hardware or their facsimiles. Allowable modifications included the addition of optical filtering and/or temporal (off-line) processing.

## APPROACH AND FOCUS

The approach to the EO Target Enhancement Program involved the following activities:

Task 1. Concept and Experiment Definition
Task 2. Procure and Modify Demonstration Hardware
Task 3. Demonstration Data Collection and Analysis

The nature of the program was focused to suggest and demonstrate implementable device modifications that could provide (1) significant performance enhancements or new capabilities at low cost, or (2) provide comparable performance at reduced cost. This focus was consistent with the program objective and was a major factor supporting the eventual selection of Low Light Level ($L^3$) and daylight visual devices as the demonstration sensors.

The program scope was limited to demonstrating one or two of the most promising phenomenological options to include (1) passive polarization enhancement, (2) multispectral discrimination, (3) spectral/temporal target cueing, and (4) Moving Target Indication (MTI) experiments. The focus on new scientific investigation, low-cost implementation, and the possible complementary enhancement concepts eliminated MTI (temporal processing only) as a demonstration candidate.

The focus on demonstrating signature exploitation concepts which could be implemented simply at low cost narrowed the phenomenological options which could be pursued. The complexity and cost of modifying existing equipments to exploit far infrared polarization signatures and/or shortwave infrared spectral signatures ruled out these phenomena as candidates for the demonstration. The phenomenological options that remained and were pursued under this program were (1) passive polarization enhancement in the visible and near infrared spectral regions and (2) spectral enhancement using near infrared target signatures.

The sensors selected for the exploitation of the target signatures were existing visual and $L^3$ sensors. For the purposes of the demonstration, an AN/AVS-6 night vision goggle set and a CCD camera were used. To exploit the signatures in a scene context, the technique selected to display suspected enhancements was to overlay modulated polarization and/or spectral signatures on directly viewed images. The concept was that modulation of these signatures on the observed scene would cue targets that would pass unobserved. For the demonstration, a dichroic polarizer was rotated in front of either the CCD camera (for daylight scenes) or the $L^3$ scope (for nighttime scenes) in order to modulate scene polarizations. To exploit the pursued spectral signature, two narrow band spectral filters were alternated in front of the aperture of the $L^3$ scope to produce a modulation created by expected differences in reflections from target surfaces.

The purpose of the demonstration test was to collect sufficient data to determine if an enhanced detection capability for $L^3$ and daylight surveillance equipment could be obtained using the overlaid polarization and/or spectral signatures. The intent was to test against various targets and backgrounds under a variety of environmentally realistic scenarios (i.e., solar and lunar illumination levels and geometries) in order to obtain a first order assessment of the capability of these signatures to improve target detection. Because of the limited scope of the program, testing under differing weather conditions was constrained to opportunities available during a single week test session.

A qualitative comparison and quantitative analysis approach fulfilled the demonstration objective. A comparison of conventional versus enhanced imagery was used as a first order utility assessment. Originally, the test plan required data to be collected from a sufficiently long target-sensor range and/or with targets in backgrounds sufficiently cluttered so that the utility of the "cues" could be assessed. However, the sites available did not allow for long-range viewing or optimal placement of the vehicles. Therefore, quantitative image metrics were used to extrapolate conclusions from data that were qualitatively judged to provide enhanced detection. The analyses were conducted in three steps: first, a qualitative assessment of the collected data; second, using image statistics, make quantitative assessments; and finally, summarize conclusions.

## CONCLUSIONS

The conclusions are presented at a level consistent with the program objective: to examine and evaluate specific physical phenomena and assess the possibility of exploiting the phenomena to enhance the performance of existing man-in-the-loop electro-optical RSTA systems. A secondary objective was to suggest and demonstrate device modifications that could provide (1) significant performance enhancements or new capabilities at low cost, or (2) provide

comparable performance at a reduced cost. Following are the conclusions with respect to the polarization and spectral signatures.

Spectral Filtering

Within the data set of this demonstration, the modulation produced by spectral filtering clearly enhanced detection performance. The enhancement was particularly noteworthy because the demonstration equipment was not optimized for the exploitation of this signature. Further investigation of this near infrared phenomenology for improved detection by direct view system is strongly recommended. However, to conduct a detailed investigation of this signature, the demonstration hardware used in this program should be modified to accommodate the indepth trade-offs necessary to optimize the enhancement. Therefore, the recommendations are (1) modify the existing demonstration equipment for the exclusive investigation of spectral filtering, (2) further data collection to validate the utility of the signature over a broad range of environmental and target conditions, and (3) develop a low cost implementation concept which optimizes the exploitation of this signature.

Polarization

As predicted, polarization target signatures were observed under a variety of illumination conditions; however, due to the sensitivity of the $L^3$ scopes used, generally the signatures were of low magnitude and appeared to have little operational utility. As the $L^3$ scopes used represent state-of-the-art, high quantum efficiency technology, there is little likelihood of near term exploitation of this enhancement. It is important to note that the conclusion drawn here applies only to direct view, visual and $L^3$ systems. The utility of polarization signatures in active systems has been demonstrated by the WES REMIDS sensor, and the utility of polarization is being studied by ERIM and others for passive sensors operation in other spectral regions.

RECOMMENDATIONS FOR PHASE II

Based on the above conclusions, further investigation of the utility of the near IR spectral characteristics of targets for performance enhancement of direct view RSTA systems is recommended. A follow-on program focused on exploiting near IR spectral signatures (with an expanded and specially tailored test program) could be conducted for nominally the same level of effort as the EO Target Enhancement Program. Ideally, such a program would take one year to allow testing in all four seasons. An analysis of the spectral signatures would be performed to optimize the filter band centers and bandwidths. Selected bands would be tested to validate performance predictions.

# 1.0 INTRODUCTION

## 1.1 PROGRAM BACKGROUND

The EO Target Enhancement Demonstration program is the outcome of an Environmental Research Institute of Michigan (ERIM) proposal under Area 1 [Reconnaissance, Surveillance, and Target Acquisition (RSTA)] of the U.S. Army LABCOM Broad Agency Announcement (BAA) dated January 1988. The program was conducted under USAE Waterways Experiment Station contract DACA39-89-K-005. The program proposed to examine and demonstrate enhancements to existing RSTA systems using target spectral, polarization, and/or temporal signature attributes not currently being exploited. In response to the BAA, ERIM proposed a two-phase effort: Phase 1, a preliminary demonstration phase (the subject of this report) that would culminate in recommendations for Phase 2, a verification demonstration phase. The stated objectives of the proposed efforts were to provide demonstrated improvements in the RSTA capabilities of conventional, ground-to-ground, man-in-the-loop, electro-optical systems, using the noted unexploited signatures of targets. To minimize the cost of the study, the demonstration hardware was constrained to include only minor modifications to existing, fielded hardware or their facsimiles. Allowable modifications included the addition of optical filtering and/or temporal (off-line) processing.

## 1.2 PROGRAM OBJECTIVE

The objective of the proposed research was to examine and evaluate the physical phenomena associated with the unexploited radiative characteristics of targets which, if exploited, would enhance the performance of man-in-the-loop, electro-optical RSTA systems. Three signature attributes currently not exploited are the spectral, polarization, and temporal aspects of these optical signals. Current RSTA systems tend to be broadband, polarization insensitive devices

where display signal-to-noise is used as the basis for the design. Exploiting polarization or spectral bandwidth generally involves collection of less energy than is available to a broadband system; however, the temporal and contextual processing power of the human operator can overcome this energy loss if the target information has been enhanced.

## 1.3 TECHNICAL HISTORICAL PERSPECTIVE

The basis for this study was established by earlier efforts conducted at ERIM in the 1970s [1,2] and at the Naval Weapons Center (NWC) in the late 1960s [3]. In the ERIM efforts, basic laboratory data provided empirical (non-imaging) evidence that polarized reflected radiance [1] and unique spectral signatures could be measured for certain target materials in the visible and near infrared spectral regions. Additionally, other efforts by ERIM [4,5] and Chrysler [6] provided evidence of polarized emission by target materials in the far infrared. Since existing RSTA devices had taken little or no advantage of either polarization or spectral signature information to enhance performance, the efforts described here investigated simple modifications for enhancement using these signatures. Early efforts by ERIM and others have shown that simple modifications to existing far infrared hardware failed to exploit polarization signatures. However, the concept of using these signatures as simple (low-cost) modifications to visible and low light level sensors remained in question. The LABCOM BAA provided the means to continue these investigations.

## 1.4 PROGRAM APPROACH AND DEMONSTRATION FOCUS

The proposed approach to the EO Target Enhancement Program (Phase 1) involved the following tasks:

Task 1. Concept and Experiment Definition: Prepare a technical justification for the study demonstration; define the

demonstration experiment and the procedures to be used to assess the performance enhancement.

Task 2. Procurement and Modification of Demonstration Hardware: In agreement with the sponsor, modify the demonstration hardware selected as part of task 1.

Task 3. Local Demonstration Data Collection and Analysis:
Task 3.1: Use the modified hardware to collect data on targets (of opportunity as a function of available weather and target operational modes.)
Task 3.2: Perform analyses of the collected data to validate the measurement procedures, to document the enhancement obtained, and to define the additional measurements necessary during the Phase 2 efforts. (A second phase will verify the robustness of the concepts by expanding the test database to include other targets, backgrounds, and environments.)

This approach was followed in the actual program execution with one exception. The local demonstration testing, Task 3, was accomplished on WES grounds in Vicksburg, Mississippi.

The initial planning activities, after contract award, quickly identified the need to establish a finite and definitive focus for the demonstration. The focus chosen and endorsed by the government program manager was to suggest and demonstrate implementable device modifications that could provide (1) significant performance enhancements or new capabilities at low cost, or (2) provide comparable performance at reduced cost. This focus was consistent with the proposed program objective and was a major factor supporting the eventual selection of low light level and daylight visual devices as the demonstration devices. A detailed discussion of the selection of the demonstration devices is presented in Section 2.0.

The proposed program scope was limited to demonstrating one or two of the most promising phenomenological options to include (1) passive polarization enhancement, (2) multispectral discrimination, (3) spectral/temporal target cueing, and (4) Moving Target Indication (MTI) experiments. (A bias toward examining polarization enhancement in the reflective portion of the EO spectrum was identified in the proposal statement of work.) The selected focus on low-cost implementation and the possible complementary enhancement concepts, discussed in the following subsection, caused the early elimination of MTI (temporal processing only) as a candidate.

## 1.5 ENHANCEMENT CONCEPT

The decision to focus the demonstration on signature exploitation concepts that could be implemented simply at low cost placed unique demands on the method of displaying the information. For example, as shown in Appendix C, polarization and/or spectral signatures alone do not provide the contextual information necessary for an operator to identify a target or establish a scene reference for the signature. This fact is also true of MTI where scenes are differenced and only the difference is displayed. Additionally, with any narrow band or polarization filtering, less energy is available to the sensor than with a broadband system. To exploit the signatures in a scene context, the technique selected to display the suspected enhancement was to overlay modulated polarization and/or spectral signatures on directly viewed images. The concept was that the modulation of these signatures on the observed scene would cue targets that would otherwise pass unobserved.

# 2.0 PHENOMENOLOGY AND DEMONSTRATION IMPLEMENTATION

## 2.1 INTRODUCTION

This section presents a review of earlier efforts conducted by ERIM to investigate unexploited target spectral, polarized, and/or temporal signature phenomenologies as potential enhancements to existing RSTA systems. The term "unexploited" is used to describe these phenomenologies because current RSTA operational systems do not use the information offered by these signatures. The hypothesis of the EO Target Enhancement program is that in some instances, it may be possible to make simple modifications to a system and provide a cost-effective means of substantially improving detection performance. A discussion on the selection criteria and final selection of the apparatus used to test this hypothesis follows the phenomenology review.

## 2.2 PHENOMENOLOGY REVIEW

Existing surveillance and target acquisition hardware takes little or no advantage of either polarization or spectral signature information to enhance detection performance. It is the objective of this research to demonstrate that simple (low-cost) modifications to visible and low light level sensors can enhance detection performance through the use of these signatures, particularly under low contrast conditions. Past efforts have shown that simple modifications to existing far infrared hardware to exploit polarization signatures are unlikely to substantially improve performance because of intrinsic polarization biases within the sensors. (Because of polarized radiation emitted by sensor optics, polarization biases tend to be severe for these devices.) For these sensors, completely new designs will probably be necessary to take advantage of polarized emission. The following phenomenology review provides the rationale for the program objective, demonstration focus, and enhancement concept

described in Section 1.0. The final selection of enhancements to be investigated under this program was made after a comparison of available (fielded) devices and unexploited signatures offering potential for enhanced performance.

### 2.2.1 Reflectance: Color and Polarization Phenomena

Manufactured objects generally are smooth and exhibit both a specular and a diffuse reflection component. Object color is carried to a great part in the diffuse component (See Figure 2-1). The spectral reflectance curves were measured at a fixed geometry (normal source incidence and receiver aspect of 50 degrees) for parallel and crossed linear polarization source and receiver conditions. Both of the measured curves show the same spectral dependence. If the crossed polarization spectra is subtracted from the parallel spectra, then the resultant curve (the pure polarization or specular component) shows less spectral content; that is, it is more white. Figure 2-2 shows data similar to Figure 2-1 except that the data were collected at a specular geometry (the source and receiver were both at 55 degrees). It can be seen that these data show the same trends. The pure polarization components (parallel minus cross) tend to be more white. For the specular geometry the perpendicular component is two orders larger than the parallel component. The point is that color is provided mainly by the diffuse, unpolarized reflection component. This implies that the color of the surface will be a function of the viewing and source geometry. Because the natural environment does not provide spatially uniform spectral illumination, it is impossible to completely match all surfaces of a three-dimensional object spectrally to the background. Thus, by using spectral filtering techniques, it should be possible to cue the contrast of certain surfaces of an object to provide enhanced detection capabilities.

Comparison of the polarization components of the data in Figure 2-2 shows the use of polarization processing. The polarization

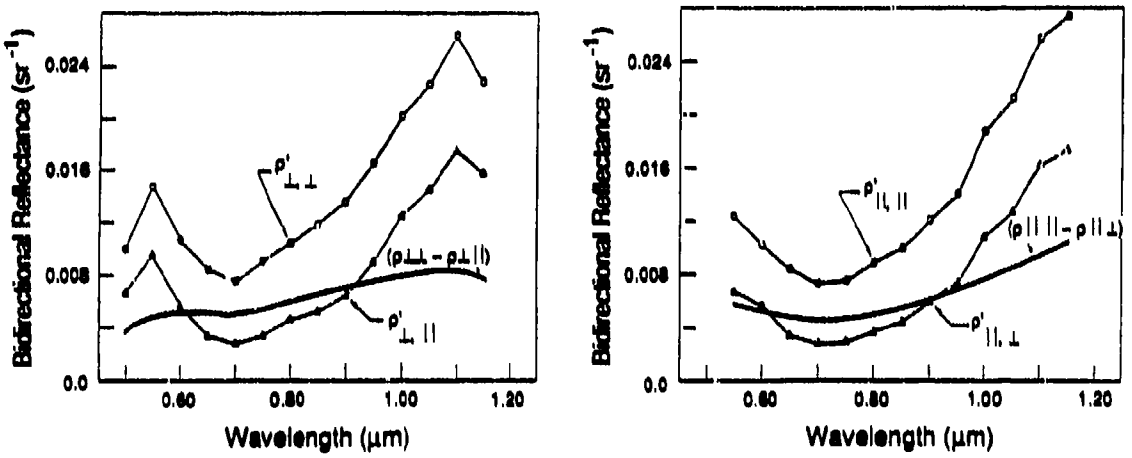


(a) Source Polarization ⊥ (b) Source Polarization ||

Figure 2-1. Spectral Bidirectional Reflectance for Green Paint for Normal Incidence and $\theta_r = 50°$

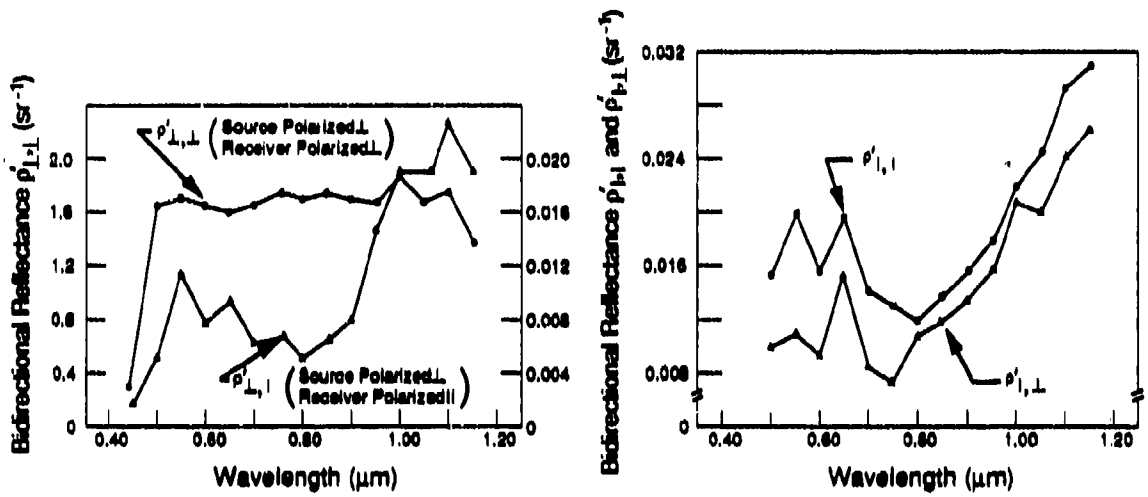


(a) Source Polarization ⊥ (b) Source Polarization ||

Figure 2-2. Spectral Bidirectional Reflectance for Green Paint (Sample No. 1027) for a Specular Geometry Where $\theta_i = 55° = \theta_r$

modulation (the difference between the two parallel source and receiver conditions), which is present at the specular geometry for the sample chosen, is equivalent to a 300 percent diffuse reflector, i.e., the specular glint is bright and very polarized. If the source at the specular geometry were the sun, then polarization would not be required to detect the glint because its magnitude would be adequate. It is when the glint geometry encounters a more subdued source such as "blue" sky in the foreground that the enhancements available using polarization could become more pronounced.

### 2.2.2 Comparison of Background and Target Polarization

Figure 2-3 shows the bidirectional reflectance of olive drab paint on metal at 0.63 μm for source angles of 40 and 60 degrees. The four curves show the reflectance measured with the source and receiver polarizers set in line with the plane of incidence (o); source and receiver polarizers set orthogonal to the plane of incidence (x); and source and receiver polarizers crossed (+ and Δ). Note that for grazing angles of incidence, there is a substantial difference between the two orthogonally polarized reflectances (o and x). For a forward-looking visible or low light level sensor, many target surfaces exhibit similar grazing angle effects. Thus, if one were to rotate a polarizer in front of a sensor, many target surfaces would flicker on the display, providing a cue to the location of the target.

Most vegetative backgrounds, on the other hand, exhibit little or no polarization. This is because leaf angles have quasi-random orientations, and subsequently, polarization induced by one leaf is often cancelled by polarization induced by other leaves. Figure 2-4 shows the bidirectional reflectance of grass on sandy soil under geometries similar to those used for the data shown in Figure 2-3. Note the small difference between the orthogonally polarized reflectances.

Figure 2-5 illustrates far infrared polarization data collected by Chrysler [6]. The four subimages illustrate the phenomenology (the

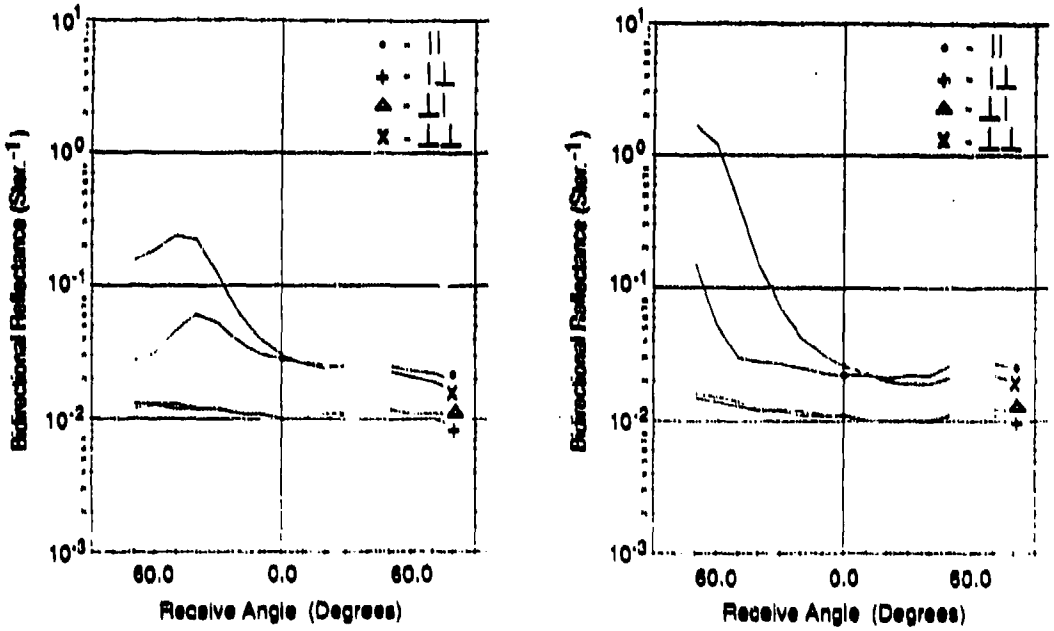


Figure 2-3. Bidirectional Reflectance of Olive Drab Paint

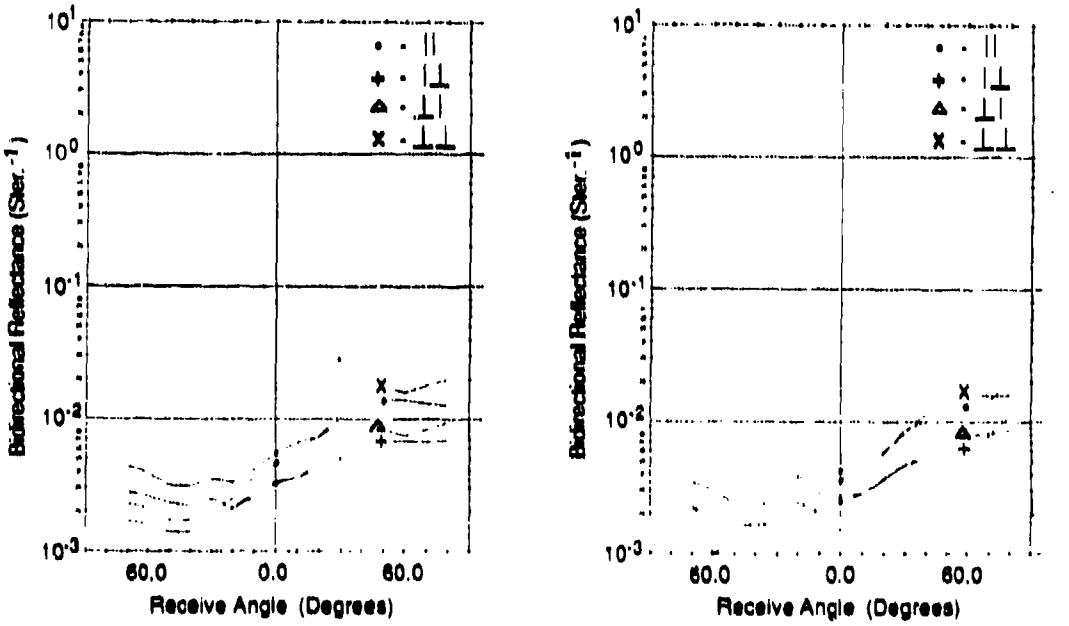


Figure 2-4. Bidirectional Reflectance of Grass on Sandy Soil

polarized emittance); a visual realization of the scene; an infrared portrayal of the scene; and the polarized content (the difference between the vertical and horizontal linear polarizations) of the scene. Two important observations should be made: (1) the polarized content occurs only for those portions of the target at the appropriate geometry (the polarized target content does not produce a total image because of the sensitivity of the instrument used to measure the data shown), and (2) the background clutter in the polarized image was reduced to the pixel-to-pixel noise of the sensor (which in the case of the Chrysler instrument was on the order of a few degrees centigrade; that is, the spatial clutter content was reduced below the sensor noise). Similar results are anticipated in the visible and near infrared region. However, because there is no substantial emission in the visible and near infrared, results are expected to be less dependent on environmental conditions (i.e., sky and target apparent temperatures) and more dependent on natural illumination levels.

### 2.2.3 Spectral Cueing

Cues for target detection can also come from spectral information. Figure 2-6 shows a composite of spectral reflectances for various olive drab paints. Figures 2-7 through 2-10 show composite spectral reflectances from grass, deciduous vegetation, coniferous vegetation and dead vegetation. Note that the live vegetation exhibits absorption bands at approximately 1.5 and 2.0 $\mu$m, which are not exhibited by the olive drab paints. Also the sharp cut-on in reflectance in the near infrared for many of the olive drab paints occurs at a somewhat longer wavelength (0.75 $\mu$m versus 0.7 $\mu$m) than the similar characteristic for live vegetation. Dead vegetation exhibits a less abrupt change in reflectance across the same region.

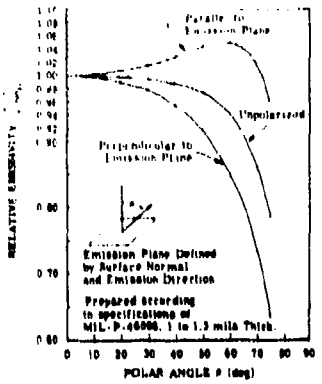


Polarized Emittance for O.D. Paint on Steel (9.96 μm)

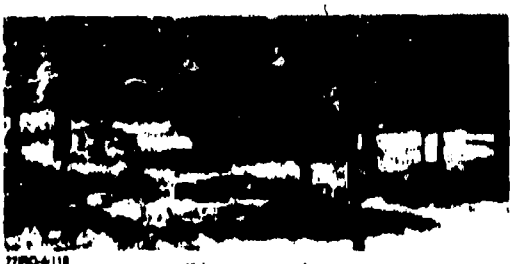

Photograph


Polarization Difference V-H

Thermal Image

90-066 R1

Figure 2-5. Polarization Enhancement

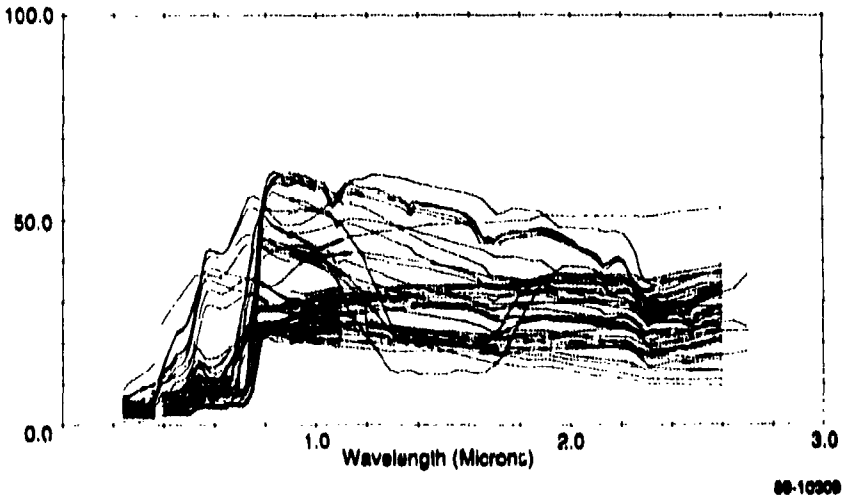


90-10309

Figure 2-6. A Composite of Spectral Reflectances Measured From Various Olive Drab Paints

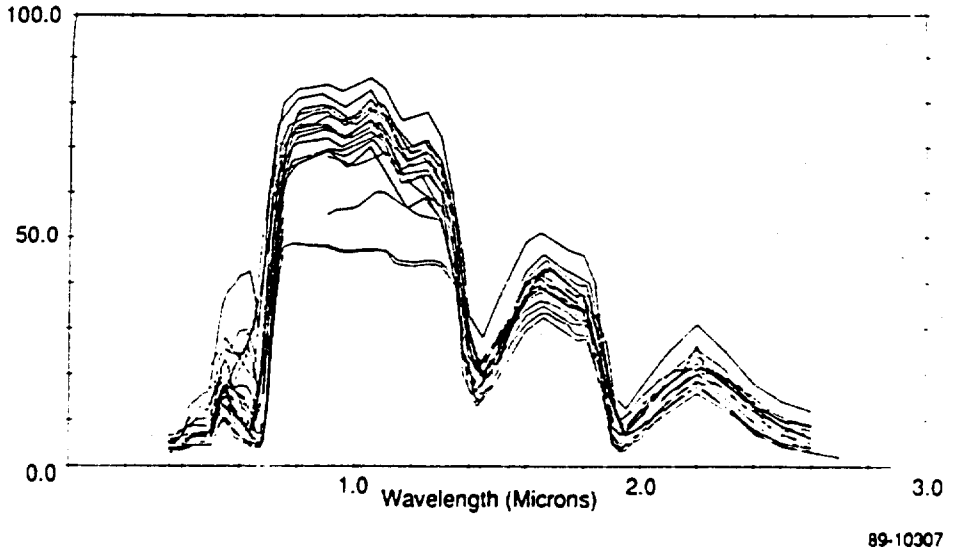


Figure 2-7. A Composite of Spectral Reflectances Measured From Various Grasses

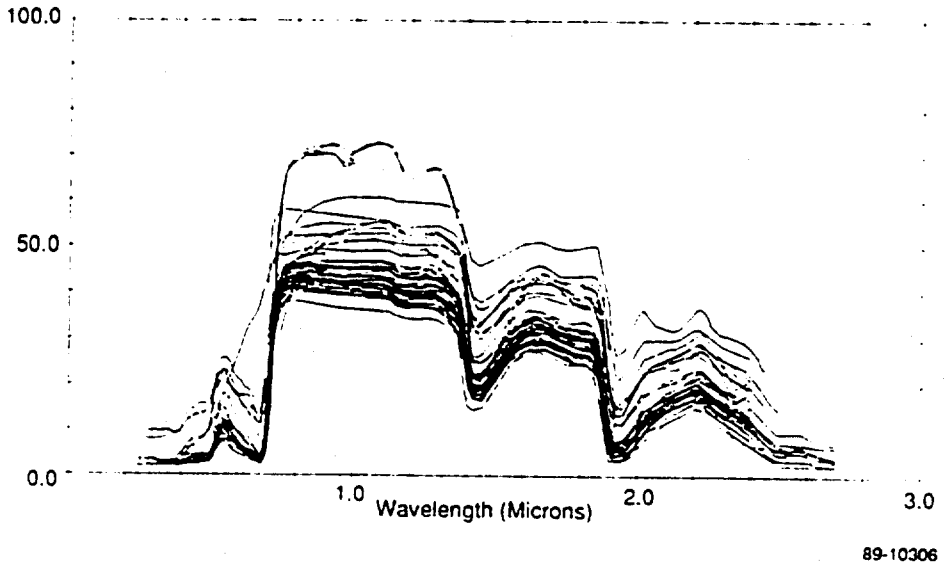


Figure 2-8. A Composite of Spectral Reflectances Measured From Deciduous Vegetation

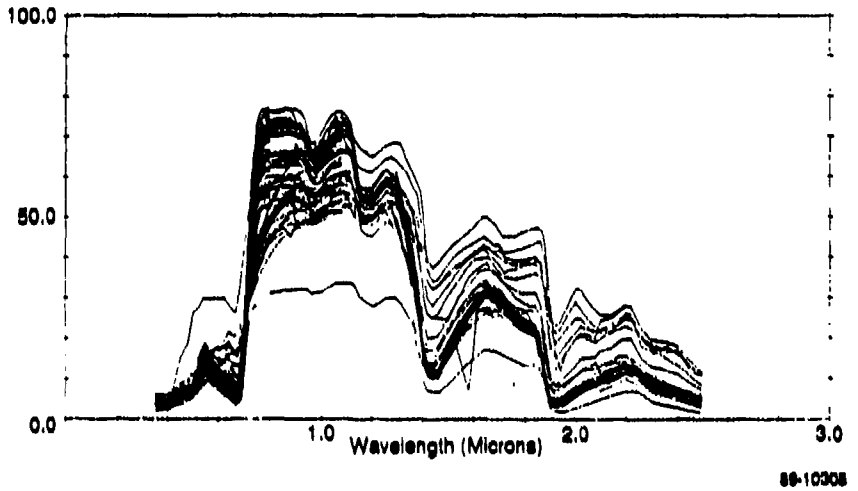


Figure 2-9. A Composite of Spectral Reflectances Measured From Coniferous Vegetation

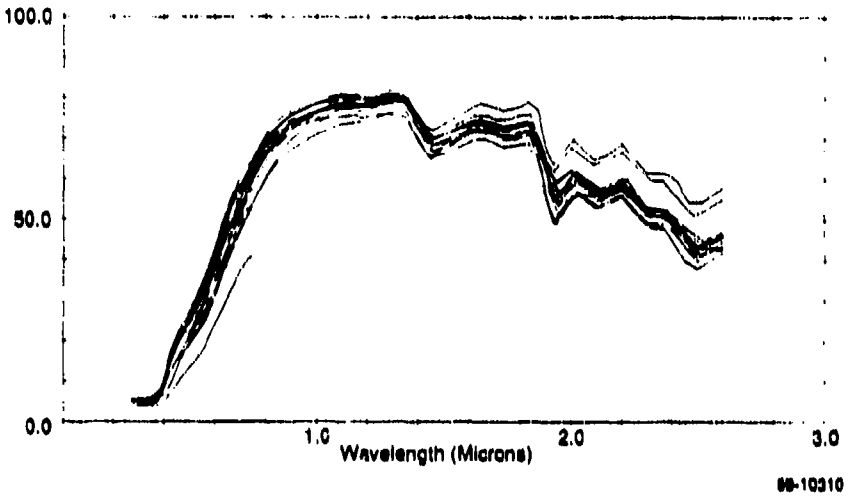


Figure 2-10. A Composite of Spectral Reflectances Measured From Dead Vegetation

Using a sensor that has been filtered to a narrow spectral band at these wavelengths may show contrast between a target and its background when little or no contrast is available for a broadband sensor. Spectral band ratioing in postprocessing may also provide a useful target detection signature.

### 2.2.4 Target Motion

Motion has been a powerful target discriminate for many years. In many situations, a target can be moving very slowly within the field of view of a sensor. (A low-contrast target may not be easily recognized, and there may be a failure to detect the target.) The aperture of such targets does occlude background signals, and the use of frame-to-frame differencing can produce a detectable difference signal. Thus by differencing sequential images, a cue may be generated indicating the motion of the target. Although the target may not be detectable by an observer, this Moving Target Indication (MTI) can provide a cue that will enhance detection. Usage of MTI is well understood; it is used in existing systems, and requires image processing and subsequent image differencing (not simple or low cost). Because this demonstration program was to focus on simple, low-cost enhancement techniques, and because techniques using polarization and spectral filtering have not been investigated, it was determined that the program should pursue the areas that provide the most new information; hence, MTI was eliminated under this demonstration program.

## 2.3 DEMONSTRATION DEVICE SELECTION

The analysis to select Low Light Level ($L^3$) and visible range sensors to demonstrate possible EO enhancements included both technical and operational considerations. The table in Figure 2-11

| | REFLECTIVE | | | THERMAL | |
|---|---|---|---|---|---|
| | Visual 0.4 - 0.7 μm | NIR 0.7 - 1.4 μm | SWIR 1.4 - 3.0 μm | MIR 3.0 - 5.0 μm | FIR 8.0 - 12 μm |
| **Phenomenology** | | | | | |
| Polarization | X | X | X | X | X |
| Spectral | | X | X | | X |
| Temporal | | | | X | X |
| **Devices** | | | | | |
| Visual | ← | — | | | |
| $L^3$ Viewers | ← | — | — | | |
| Elect. Viewers | | | | ← | — → |

Figure 2-11. Signature and Device Overview

shows the applicability of the phenomenologies discussed in Section 2.2 and the operating range of various inventory viewing devices for common EO spectral bands. The term "Electronic Viewers" refers to framing infrared sensors or FLIRs. With the elimination of temporal processing from consideration as discussed in the previous section, this table indicates that $L^3$ and visible range devices and long wavelength FLIRs would best support program objectives. Existing FLIRs exhibit complex polarization biases while $L^3$ devices exhibit little or no polarization biases. While several attempts have been made to modify existing FLIRs for scene polarization measurement, the results of these attempts have been less than satisfactory. From an operational perspective, FLIRs are commonly installed in vehicles as part of a weapon delivery system; whereas, $L^3$ devices can be considered individual personnel RTSA equipment. Improved target detection is viewed as operationally advantageous to both devices. The unavailability of a FLIR with small polarization biases and the cost of modifying such a FLIR, however, eliminated this type of device as a candidate demonstration sensor; $L^3$ and visible range devices were consequently selected as the demonstration sensors. The selection and modification of the test equipment is discussed in the following section.

## 2.4 TEST EQUIPMENT DESCRIPTION

The test equipment was comprised of a test sensor pallet (on which the CCD video cameras, $L^3$ scopes, and a rotating mechanism were mounted), two video monitors and two 3/4 inch video tape recorders. These were powered in the field using a 3 kW regulated generator. Portions of the test equipment are shown with a video waveform monitor in Figure 2-12.

The sensor pallet was constructed so that it could be easily reset in the field for either polarization or spectral tests and for either daylight or nighttime illumination. The baseline pallet consisted of

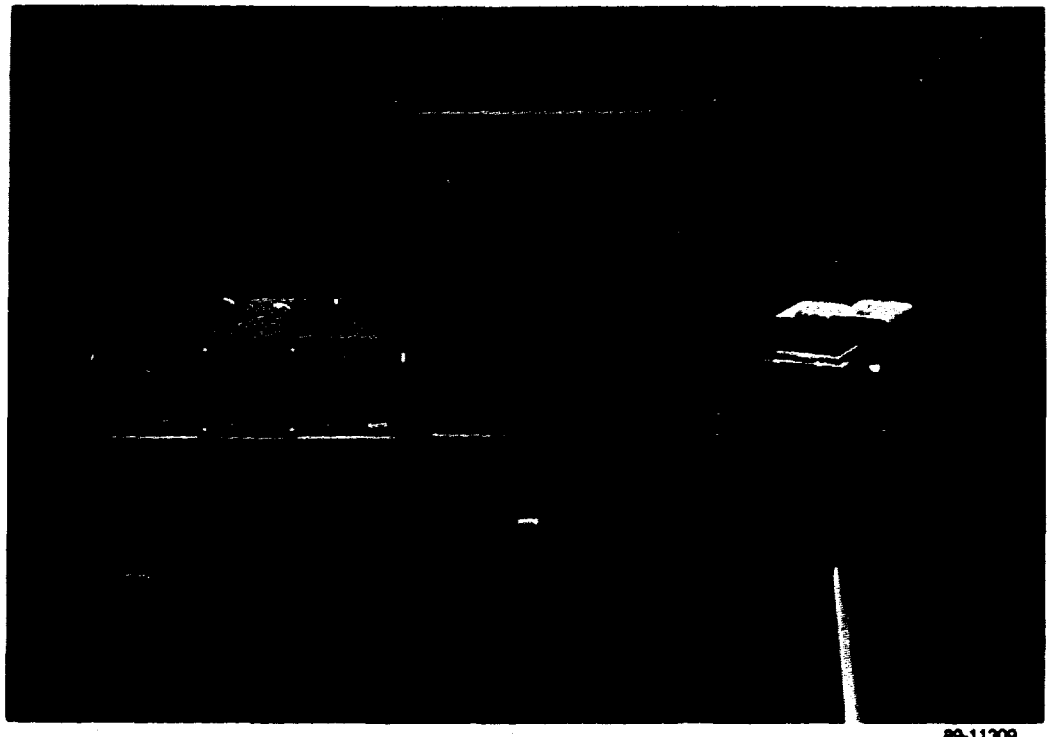

89-11309

Figure 2-12. Test Equipment

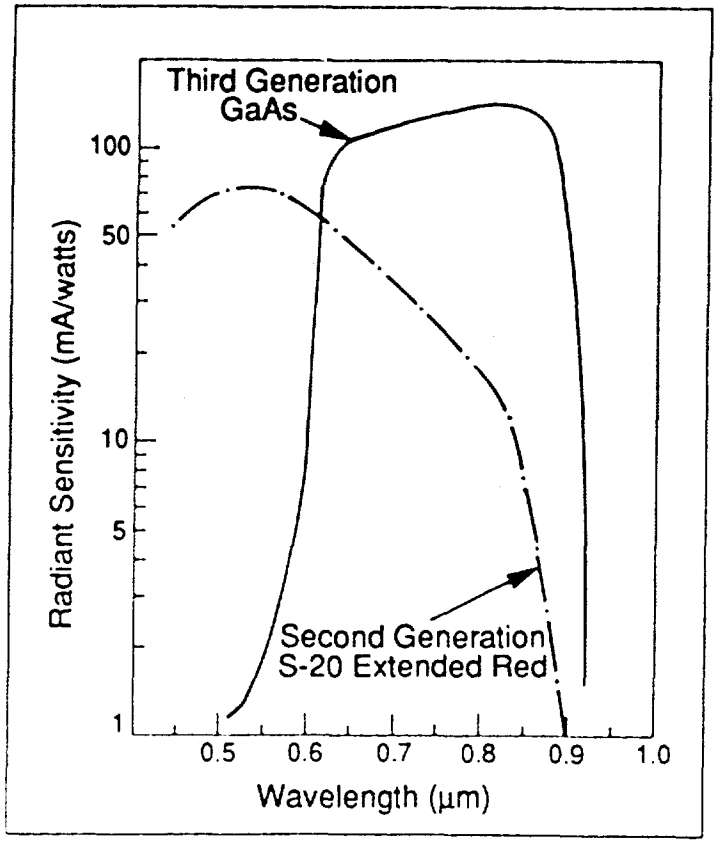


89-10314

Figure 2-13. Typical Radiant Sensitivity of 2nd and 3rd Generation Photocathodes

two Javelin JE-7262 CCD video cameras for converting daylight scenes and/or the image output of the low light level scopes to a video signal which could then be recorded on tape. These cameras were chosen because of their relatively high sensitivity (0.04 lux minimum faceplate illumination) which was necessary to sense the dim output of the scopes under starlight conditions.

The low light level scopes were a pair of image intensifier/lens assemblies that had been removed from an aviator night vision goggle set (AN/AVS-6). The intensifiers were generation III tubes having gallium arsenide photocathodes and microchannel plate construction. This intensifier was selected because its high sensitivity represents the state-of-the-art, low light level, reflective band sensors. Figure 2-13 compares the spectral radiant sensitivity of the generation III and generation II image intensifiers.

For polar enhancement, a dichroic polarizer was placed in a rotation mount in front of the sensor (either the low light level scope or the CCD camera). The mount for the polarizer was rotated by a friction drive (a 3.3 cps synchronous AC motor) through a variable ratio transmission. The transmission was continuously variable in ratio from 4:1 to 1:4, allowing rotation rates of 0.83 to 13.2 cps. The range of available polarization cycling rates was consequently 1.66 to 26.4 Hz. The pallet configuration, using the dichroic polarizer, is shown in Figure 2-14.

Spectral band switching for enhancement was performed using the same rotating assembly as for the polarizer. Two narrow band spectral filters, one with a center wavelength of 0.7 $\mu$m, the other with a 0.85 $\mu$m center wavelength, were attached to a fixture on the rotating assembly. By offsetting the rotational axis of the mount, the sensor would view the scene alternately through each filter, once per cycle of the mount. This allowed cycling rates of 0.83 to 13.2 Hz. The transmission of the filters was adjusted by adding neutral density filters to the fixture until the intensity of background vegetation

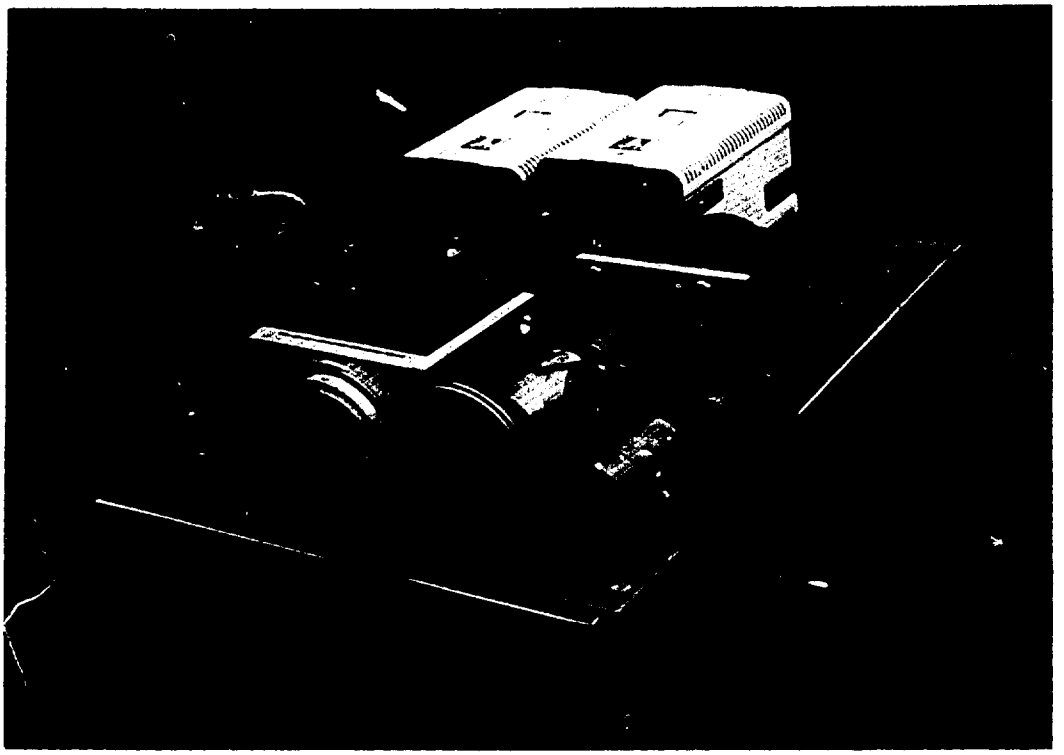

89-11308

Figure 2-14. Pallet Configuration Using Dichroic Polarizer

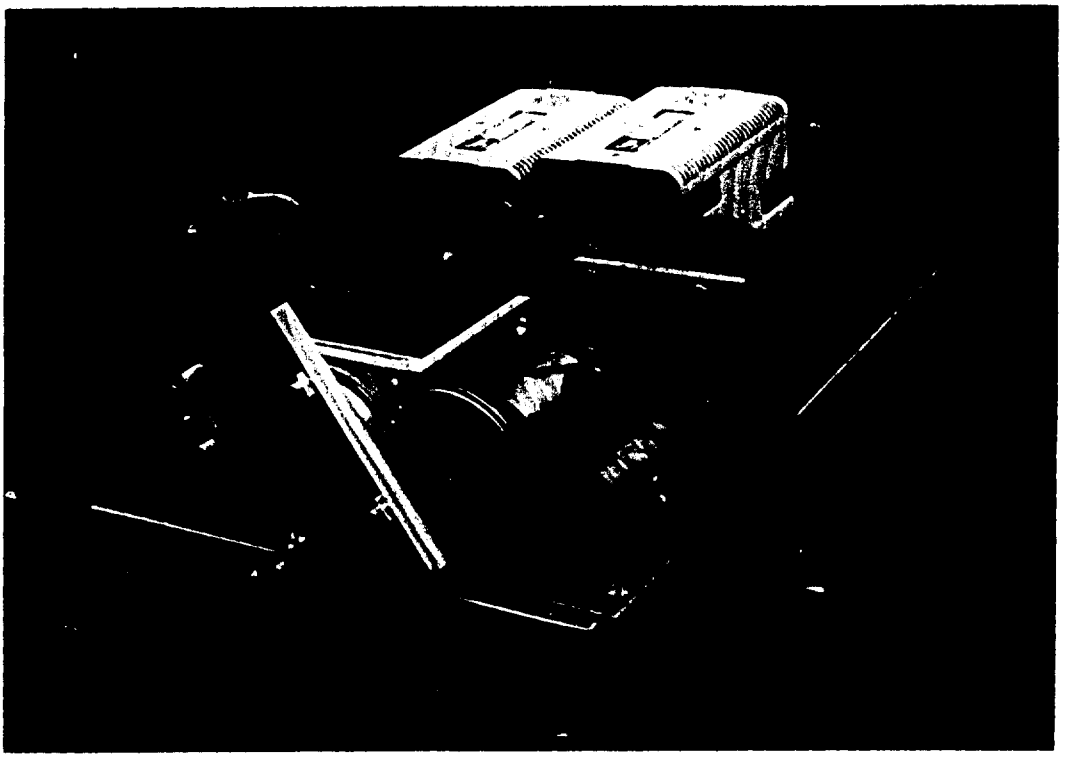

89-11307

Figure 2-15. Pallet Configuration Using Spectral Filters



**Preceding Page Blank**

did not modulate. The selection of the filter center wavelengths and bandwidths was somewhat arbitrary in that, readily available, off-the-shelf, filters were used. However, the filters chosen were selected in order to sense spectral bands where, in one case, there is a large difference between the reflectances of OD paint (0.7 $\mu$m), and in the other case, where there is little difference in the two reflectances (0.85 $\mu$m). Adjustment for total scene brightness was accomplished through the incorporation of slots for neutral density filters common to both spectral filters and a continuously variable iris between the rotating mount and the sensor. The pallet configuration using the spectral filters is shown in Figure 2-15. The relative spectral transmission of the two filters are shown in Figure 2-16.

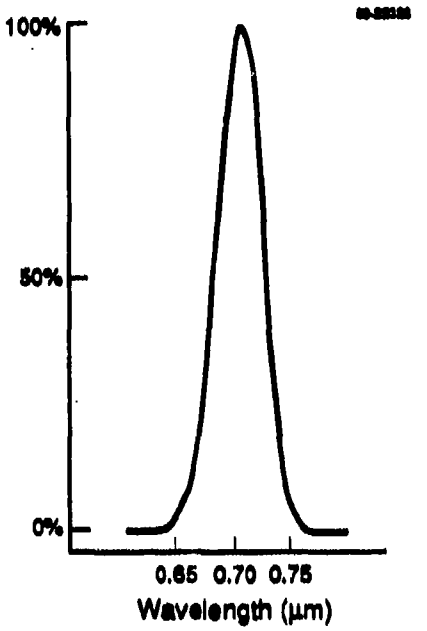


(a) 0.7 μm Spectral Filter

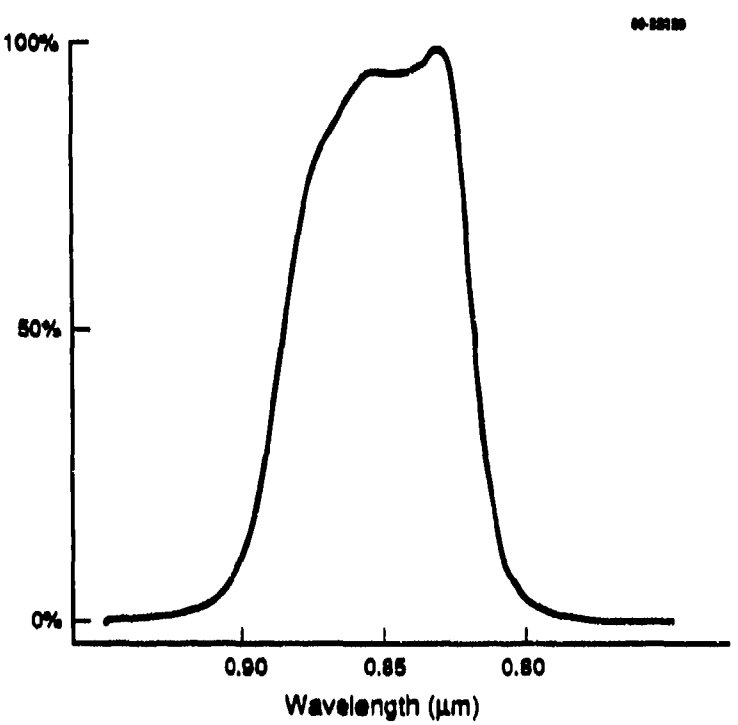


(b) 0.85 μm Spectral Filter

Figure 2-16. Relative Spectral Transmission of Filters

## 3.0 DEMONSTRATION TEST

The goal of this program was to demonstrate enhanced detection capability for low light level and daylight surveillance equipment using overlaid polarization and/or spectral signatures on the directly viewed images to cue targets that might otherwise pass unobserved. The purpose of the demonstration test was to collect sufficient data to determine if that goal had been achieved. The intent was to test against various targets and backgrounds under a variety of environmentally realistic scenarios (i.e., solar and lunar illumination levels and geometries) where each signature phenomenology pursued could be assessed as to its capability to significantly improve target detection. Because of the limited scope of the program, testing under differing weather conditions was limited to opportunities available during a single one week test session.

### 3.1 TEST SITE DESCRIPTION

A number of candidate test sites were considered. Site selection was based on the availability of a variety of military vehicles, availability of suitable natural background terrains within a reasonable distance of the vehicle depot, the cost for performing the test at each location, and the lead time required to gain permission to use the vehicles and sites for this test. Based on these criteria, it was decided to conduct testing at the Waterways Experiment Station compound in Vicksburg, Mississippi.

Testing took place during the week of September 18, 1989. Selection of the specific test site location(s) was performed upon arrival of test personnel at the Station. The two terrain areas selected for testing were sufficiently far away from artificial light sources (street lights, etc.) to have scene illuminations dominated by natural sources. These areas are known as the Dredge/Fill area and

the Poor House area. The Mobility Systems Division of the Geotech laboratory at the Station provided the vehicles and the personnel to move them during the test.

The Dredge/Fill Site is shown in Figures 3-1 and 3-2. Figure 3-1 illustrates the arrangement of vehicles and observation points on September 18, and Figure 3-2 shows the site configuration on September 19 through 22. The map legend for the vehicle and test observation locations is given in Table 3-1. The vehicles were repositioned on September 19 because distant street lights interfered with testing performed on September 18. The M-1 battle tank located at vehicle position 6 was not available until September 21. This site consisted of an open grass field surrounded by a road and dense woods as shown in the photograph from observation point 6, Figure 3-3a. Although it was intended to partially obscure the vehicles by placing them under the edge of the wooded canopy, this was not possible because of a large drainage ditch between the road and woods.

The Poor House Site is shown in Figure 3-4. The legend for the vehicle and test observation locations is given in Table 3-2. In addition to being well away from artificial lighting, this site offered a more natural wooded background as seen in the photograph from observation point 7, Figure 3-3b. This site was more confined than the Dredge/Fill site, allowing only two vehicles to be emplaced without overcrowding the vehicles. The maximum range that could be achieved without completely obscuring the test targets was about 150 yards. The M-2 Bradley fighting vehicle was repositioned from vehicle position 11 to position 12 because the first position was too far under the wooded canopy to be viewed from the test observation point. The 2 1/2 ton truck located at position 10 was heavily obscured by brush when viewed from the observation point. No attempt was made to move this vehicle because it was in disrepair and had to be towed; an adequate variety of vehicles was available without the use of the truck.

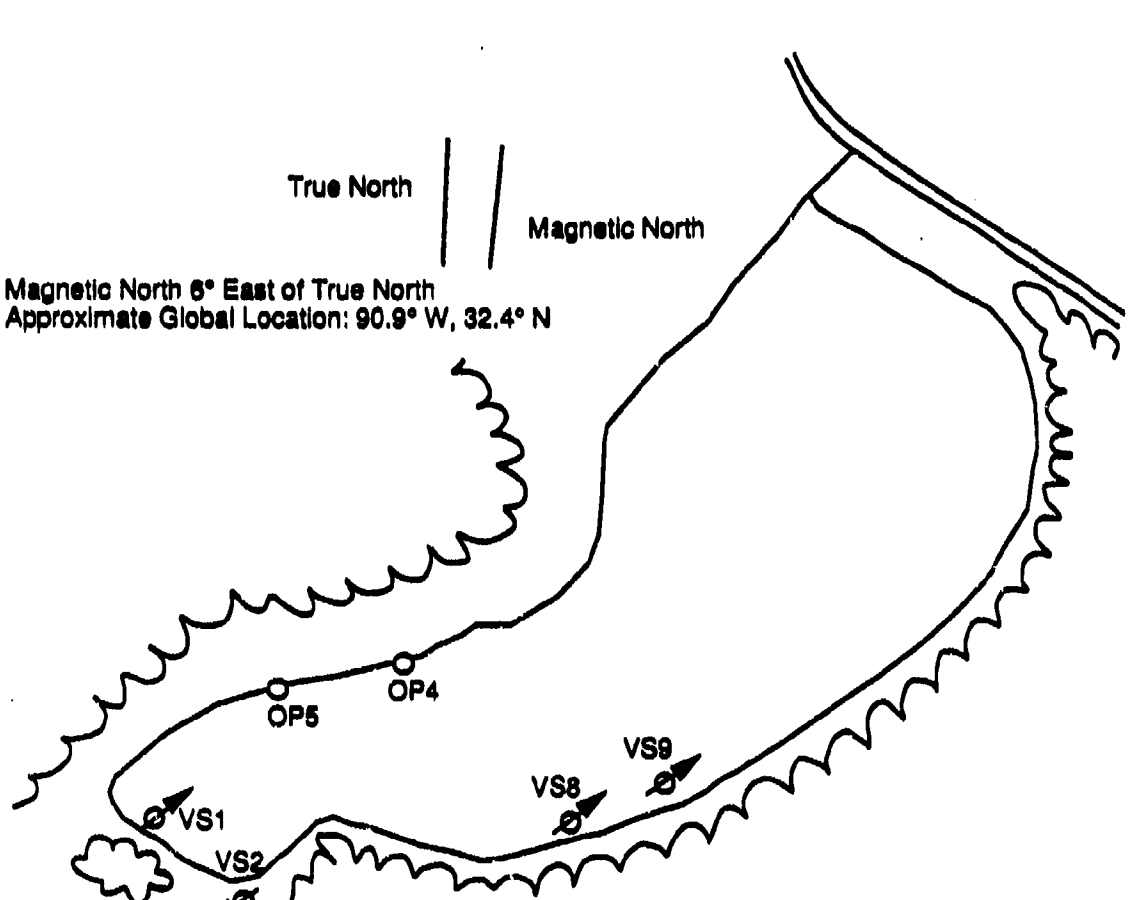


Figure 3-1. Dredge/Fill Site 18-19 September

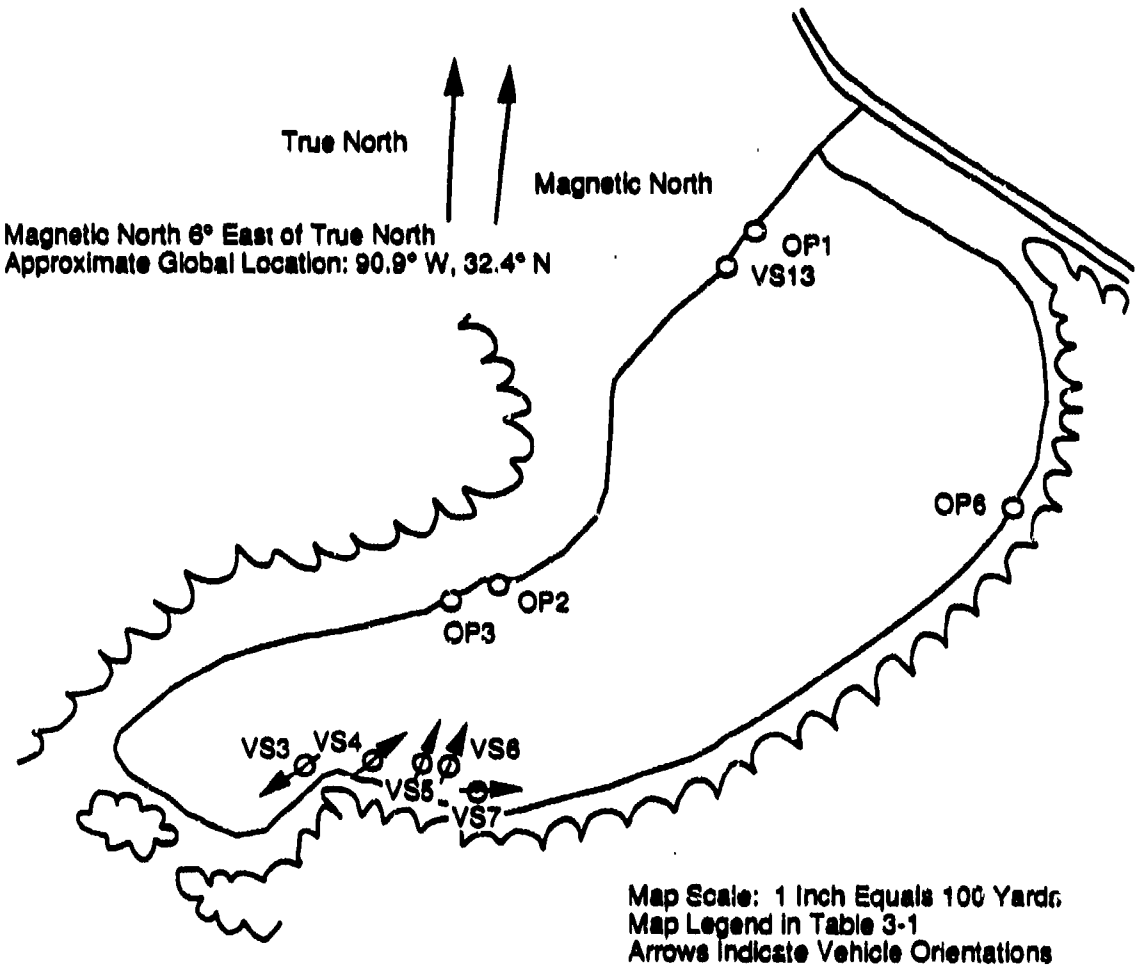


Figure 3-2. Dredge/Fill Site, 19-22 September

TABLE 3-1. DREDGE/FILL TEST AREA MAP LEGEND

Map Scale: 1 inch equals 100 yards

Magnetic North 6° East of True North

Approximate Global Location: 90.9° W, 32.4° N

Map Legend:

Observation Points:

OP1: Observation Point 1
OP2: Observation Point 2 (One Way Sign)
OP3: Observation Point 3
OP4: Observation Point 4 (Telephone Pole)
OP5: Observation Point 5
OP6: Observation Point 6

Vehicle Sites:

VS1: Vehicle Site 1 (M-113 APC), 18-19 September
VS2: Vehicle Site 2 (M-60 Tank), 18-19 September
VS3: Vehicle Site 3 (M-60 Tank), 19-22 September
VS4: Vehicle Site 4 (M-113 APC), 19-22 September
VS5: Vehicle Site 5 (M-151 Jeep), 19-22 September
VS6: Vehicle Site 6 (M-1 Tank), 21-22 September
VS7: Vehicle Site 7 (Soviet ZIL), 19-22 September
VS8: Vehicle Site 8 (Soviet ZIL), 18-19 September
VS9: Vehicle Site 9 (M-151 Jeep), 18-19 September
VS13: Location of Three M-15 Anti-Vehicular Mines Painted with CARC 383 O.D.

(a) Dredge/Fill Site

89-11645-8

(b) Poor House Site

89-11643-11

Figure 3-3. Test Sites

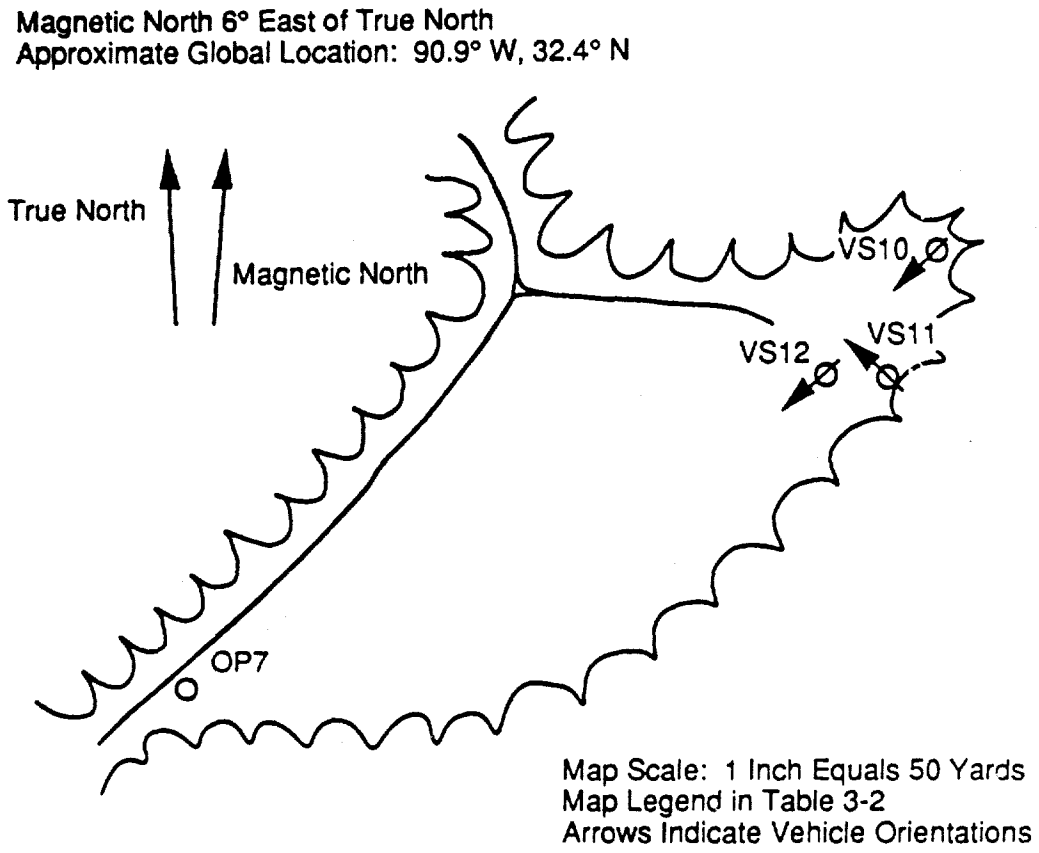


Figure 3-4. Poor House Site, 18-22 September

**Preceding Page Blank**

TABLE 3-2. POOR HOUSE TEST AREA MAP LEGEND

Map Scale: 1 inch equals 50 yards

Magnetic North 6° East of True North

Approximate Global Location: 90.9° W, 32.4° N

Map Legend:

OP7: Observation Point 7
VS10: Vehicle Site 10 (2 1/2 Ton Truck), 18-22 September
VS11: Vehicle Site 11 (M-2 Bradley), 18-19 September
VS12: Vehicle Site 12 (M-2 Bradley), 19-22 September

## 3.2 VEHICLE DESCRIPTION

The vehicles used for the test included an M-113 APC, an M-60 tank, an M-151 jeep, an M-2 Bradley, an M-1 Abrams tank, a 2 1/2 ton truck and a Soviet ZIL truck. Close-up photographs of the test vehicles are shown in Figures 3-5 through 3-11. Several inert M-15 anti-vehicle mines were also used during the test (see Figure 3-12).

All of the vehicles, with the exception of the Soviet ZIL, were painted with various shades of olive drab. The M-60 tank and 2 1/2 ton truck had patches of brown paint in addition to the olive drab. The surfaces of the M-1 tank and the M-2 fighting vehicle were also intentionally roughened, using a sand or metal particle paste, to create a diffusely reflecting surface. The Soviet ZIL was painted for desert operations and was sand colored.

The M-151 jeep was an older vehicle and did not have the same infrared reflective olive drab paint like the other U.S. vehicles. As a consequence, this vehicle appeared darker than surrounding vegetation when viewed with the low light level scopes because of the infrared sensitivity of these devices; in comparison, the other vehicles painted olive drab appeared to reflect in a manner similar to vegetation when viewed with the scopes. The specific paints used on the vehicles and their actual spectral characteristics were not known by the organization maintaining the vehicles. The M-15 mines were painted with CARC 383 olive drab.

## 3.3 TEST RESULTS

Predictions for potential polarization and spectral signatures of various targets used in visual and low light level viewing devices were made before testing. The original prediction is illustrated in the chart in Figure 3-13. Only a portion of the targets and illumination conditions shown were represented during the test. Figure 3-14 shows the targets and illumination conditions present during the test.

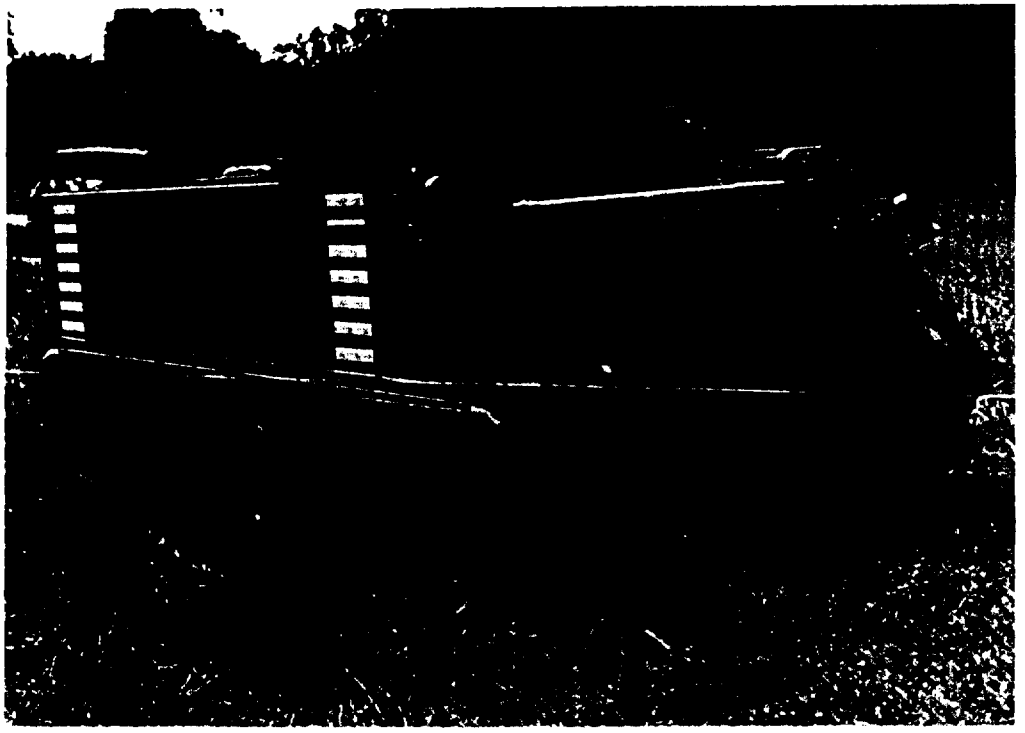

89-11643-2

Figure 3-5. M-113 APC

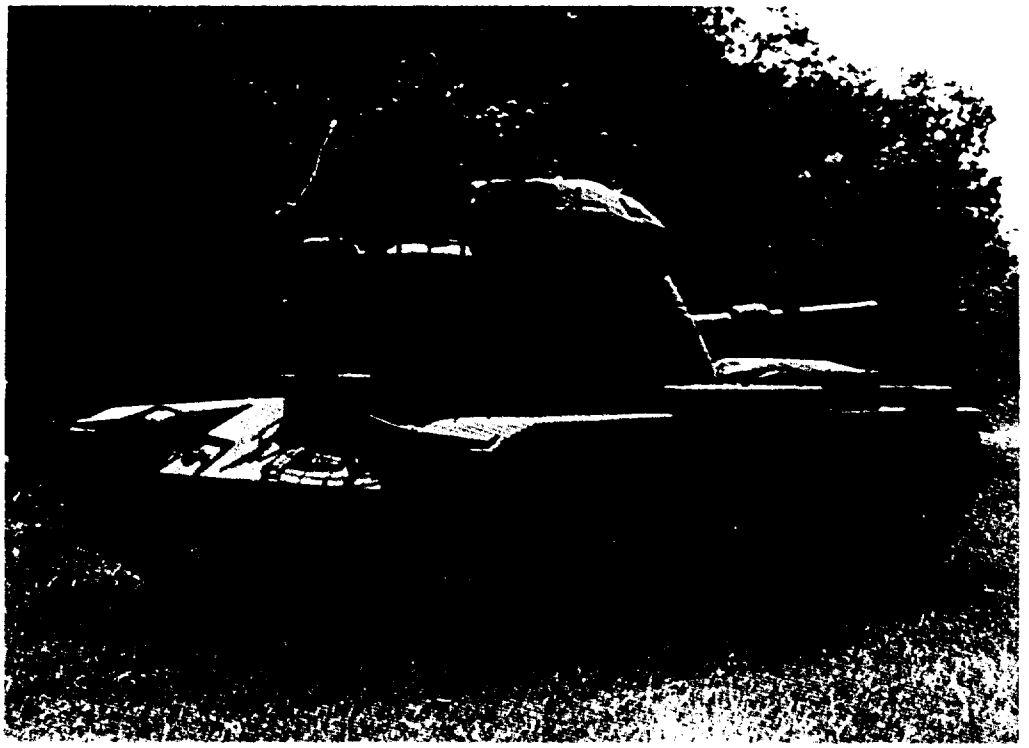

89-11643-1

Figure 3-6. M-60 Tank

89-11643-4

Figure 3-7. M-151 Jeep

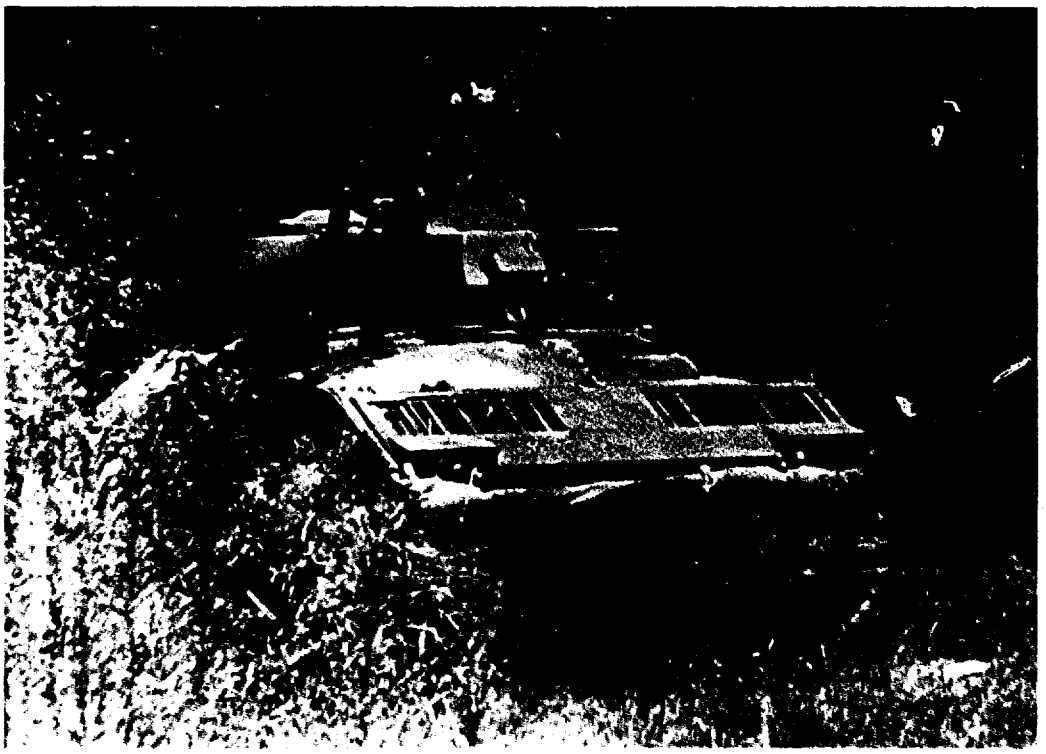

89-11643-13A

Figure 3-8. M-2 Bradley IFV

**Preceding Page Blank**

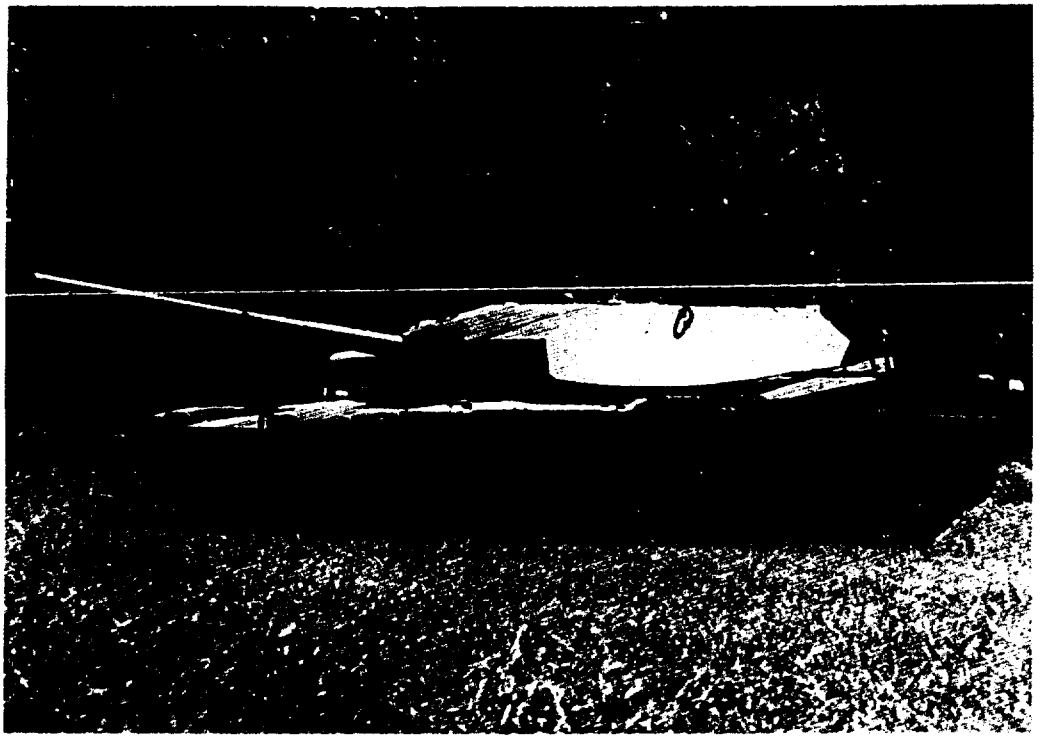

89-11645-4

Figure 3-9. M-1 Abrams Tank

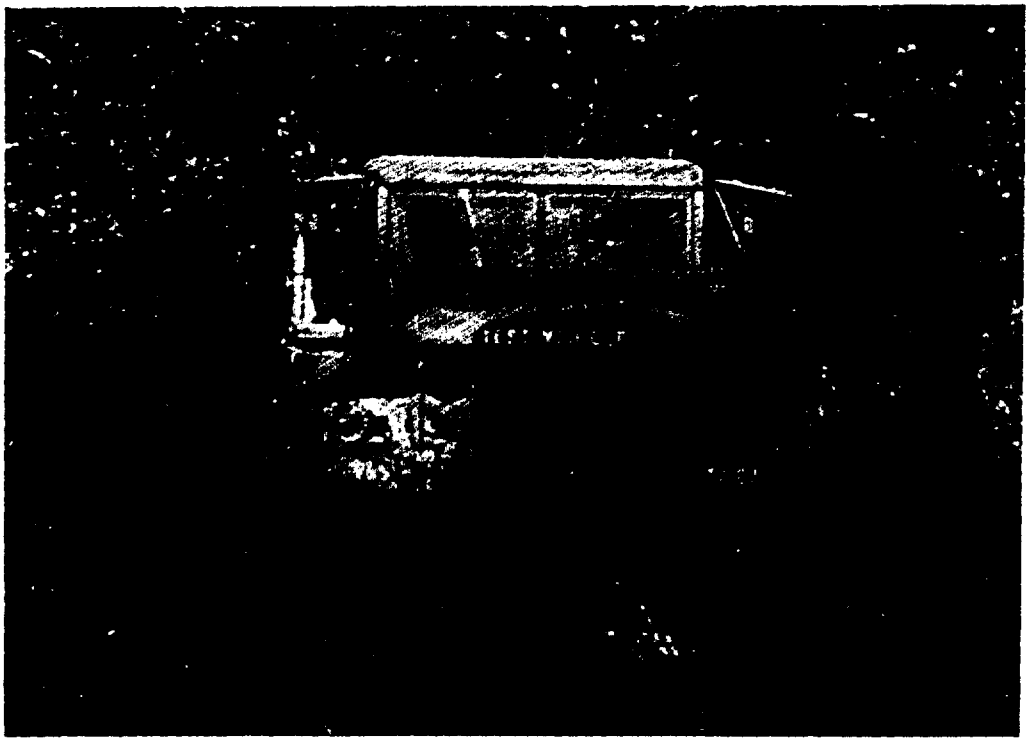

89-11644-2

Figure 3-10. 2 1/2 Ton Truck

**Preceding Page Blank**

89-11643-7A

Figure 3-11. Soviet ZIL

89-11644-16

Figure 3-12. M-15 Anti-Vehicle Mine

**Preceding Page Blank**

89-20408 R1

| Conditions \ Targets | Ground Vehicles | | Surface Mines | | Personnel | | Low Level Helicopters | | Camouflage | |
|---|---|---|---|---|---|---|---|---|---|---|
| | Polar | Spect | Polar | Spect | Polar | Spect | Polar | Spect | Polar | Spect |
| Sunlight | | | | | | | | | | |
| Clear | L | L | L | L | P | P | L | L | P | P |
| Overcast | L | L | L | L | P | P | L | L | P | P |
| Lunar | | | | | | | | | | |
| Full Moon | | | | | | | | | | |
| Clear | L | P | L | P | P | P | L | P | P | P |
| Overcast | L | U | L | U | P | U | L | U | P | U |
| Quarter Moon | | | | | | | | | | |
| Clear | L | P | L | P | P | P | L | P | P | P |
| Overcast | L | U | L | U | P | U | L | U | P | U |
| Starlight | | | | | | | | | | |
| Clear | L | U | L | U | P | U | L | U | P | U |
| Overcast | P | U | P | U | U | U | P | U | U | U |

**L - Enhancement Likely**
**P - Enhancement Possible**
**U - Enhancement Unlikely**

Spectral at 0.70 μm
Polarization at 0.4 to 0.9 μm

Figure 3-13. Estimated Enhancement Potential

89-22330

| Conditions \ Targets | Ground Vehicles | | Surface Mines | | Camouflage Net | |
|---|---|---|---|---|---|---|
| | Polar | Spect | Polar | Spect | Polar | Spect |
| Sunlight | | | | | | |
| Clear | * | | * | | | |
| Overcast | * | * | | * | * | * |
| Twilight | | | | | | |
| Clear | * | | | | | |
| Overcast | * | | * | | | |
| Lunar | | | | | | |
| 72% Disk (Clear) | * | | | | | |
| 64% Disk (Clear) | * | | | | | |
| Starlight | | | | | | |
| Clear | * | * | | | | |

Figure 3-14. Targets and Conditions Tested

The test scene was viewed using both filtered and unmodified sensors simultaneously (described in Section 2.0). We expected the overlaid cues to show a blinking effect from light amplitude modulation from the polarized or spectral target signature. During these observations, the output of both CCD cameras was recorded on video tape. Appendix A tabulates all pertinent information relating to each segment of the recorded raw data. This includes the local time and date at the recording began, the location the observation was made, the arrangement of filters used on the modified sensor, the modulation rate used, the vehicles viewed, the approximate line of sight to each vehicle from true north, and the approximate range. The additional comments indicate whether or not modulation of the vehicle surfaces was visually apparent. Daylight photographs of the test targets viewed from the primary test observation points (points 1, 3, 6 and 7) are shown in Figures 3-15 through 3-18.

### 3.3.1 Low Light Polarization Tests

During the first phase of testing (September 18 through 20), the emphasis was on polarization signatures under starlight and lunar illumination. For these test observations, the rotating dichroic polarizer was used in conjunction with a low light level scope. Observations of the test vehicles were primarily made from observation points 3 and 6 at the Dredge/Fill site and at observation point 7 at the Poor House site. The sky was completely clear during these observations and illumination was provided by either starlight or the moon at various elevation angles. With one exception, slight or no modulations were observed during these tests.

Slight modulation of certain vehicle surfaces (panels, windshields, etc.) was visually noticeable (see scene numbers 2 through 15 in Appendix A) when the sensor line of sight appeared at or near the direction of the specular reflection of the source illuminating the particular surface. No visible modulation was

observed from any position when vehicles were illuminated by starlight only, or from observation point 6 where moonlight was from the same direction of the observations. The only visually strong modulation that occurred came from the side panel of the M-113 armored personnel carrier as viewed from observation point 3. This signature was caused by the specular reflection of a distant street light on the white paint stripes and glossy white stickers on the side (front and rear) of the vehicle and by reflection of the vehicle neoprene tread skirt (see Figure 3-5). The modulation resulting from polarization of moonlight by vehicle surfaces appeared weak by comparison with the modulation on the side of the M-113.

### 3.3.2 Daylight Polarization Tests

During the next phase of the test (September 20), we emphasized polarization signatures observable under daylight illumination. For these test observations, the rotating dichroic polarizer was used in conjunction with only a CCD camera. We observed the test vehicles again from observation points 3 and 6 at the Dredge/Fill site and at observation point 7 at the Poor House site. The sky was completely clear during this phase of the test and illumination came from both direct and diffuse sunlight.

The modulation resulting from polarization by certain surfaces of the M-1, M-60, M-113 and Soviet ZIL was visually apparent under all circumstances during the daytime polarization observations (see scene numbers 16 through 24 in Appendix A). Little or no modulation was visible on the jeep or M-2. Although polarization caused by daylight illumination of the vehicles appeared more substantial than the nighttime signatures, the only signature providing a particularly strong modulation was caused by the specular reflection of the sky on the glossy finish of a civilian automobile that happened to be on site during the observation of Scene 16.

89-11645-11

Figure 3-15. View From Observation Point 1

89-11644-23

Figure 3-16. View From Observation Point 3

89-11645-8

Figure 3-17. View From Observation Point 6

89-11643-11A

Figure 3-18. View From Observation Point 7

### 3.3.3 Daylight Spectral Tests

During the third and final phase of the test (September 20), we emphasized spectral signatures under daylight illumination. We mounted the two spectral filters on the rotating assembly and used them in conjunction with the low light level scopes. We observed the test vehicles from observation points 1 and 3 at the Dredge/Fill site and at observation point 7 at the Poor House site. The sky was completely overcast by a contiguous layer of clouds beginning at approximately 0700 hours and illumination was from sunlight scattered by the cloud layer.

We observed a high degree of target modulation in most cases using the spectral filters, with little or no modulation of the vegetative backgrounds. It was noted that the blackened gap between the spectral filters caused a distracting periodic blanking of the image. We could have remedied this through the use of a specially made filter; however, the cost of a one-of-a-kind interference filter was beyond the scope of this effort. It was also noted that the sky was quite bright when viewed through the 0.7 $\mu$m narrow band filter. This caused the low light level scope to saturate and, as a consequence, diminished target contrast and target modulation when the sky was within the field of view of the sensor. The visual strength of the modulation indicated that the signature has potential use for target enhancement, but the implementation used here to exploit it was inadequate.

## 3.4 ANCILLARY DATA

Ancillary data associated with each recorded test observation are also presented in Appendix A. These include the elevation and azimuth of the sun and moon in order to establish the illumination geometry of each scene. Also included is an estimate of the lunar illumination level for moonlit scenes.

The elevation and azimuth of the sun and the moon were calculated in order to obtain accurate values for these quantities. The position of the sun and moon were calculated in geocentric coordinates using the orbital elements provided by the American Ephemeris and Nautical Almanac [7]. The geocentric coordinates were then transformed into the local azimuth and elevation using local latitude, longitude and elevation above sea level. The local coordinates cited are coordinates of the centroid of each astronomical body. Appendix B presents tabulations of the azimuth and elevation of the sun and moon at each hour of local time (Central Daylight) for the data collection period, September 18 through 22. The time at which the astronomical rise or set of the sun and moon centroid occurred and the lunar phase are also listed. This table was generated in order that observation times could be efficiently planned to cover a range of illumination levels. Note that the moon was waning during the data collection period. The coordinates of the sun and moon and the lunar phase were also calculated for each time data was recorded and are presented along with other information in Appendix A.

For scenes where moonlight was the dominant illumination source, an estimate of the irradiance by the moon onto the scene is given in Appendix A. The irradiance was derived from data given by Biberman and Nudelman [8]. The spectral irradiance of the light from a full moon as given in [8] was integrated over the relative spectral response of the low light level scope (Figure 2-13) for air masses of 1 through 10 (lunar elevations of 90 degrees through 5.8 degrees). The in-band irradiance from the moon at the lunar elevation for each scene considered was then estimated by interpolating between the above 10 data points and multiplying by the fractional lunar phase.

## 4.0 ANALYSIS AND CONCLUSIONS

The approach selected to analyze the collected field data and to assess the utility of polarization and spectral enhancements was chosen from three candidate approaches established in the planning phase of the program. The three candidate approaches were (1) a quantitative signature measurement and analysis; (2) a man-in-the-loop evaluation using the displayed data; and (3) a comparison of conventional versus enhanced imagery as a first order qualitative assessment of utility. The quantitative analysis approach, although useful from a scientific standpoint, does not readily meet the needs of an assessment of direct view, man-in-the-loop surveillance/ reconnaissance systems. We recognize that to make a recommendation for operational implementation, a human factors, man-in-the-loop evaluation and verification of statistically significant data is necessary. While a man-in-the-loop assessment approach was considered highly desirable because of the amount data and manpower required, it was decided that the man-in-the-loop analysis approach was beyond the demonstration level and scope of the program. The qualitative comparison approach of conventional versus enhanced sensor detection performance was selected as the approach that best fulfilled the demonstration objective within the scope of the program, and if significant performance enhancement was exhibited, a second phase verification program, as proposed, would be performed.

Originally, the test plan called for data to be collected from a sufficiently long target-sensor range and/or with targets in backgrounds sufficiently cluttered so that "cues" could be assessed by test personnel to provide enhanced detection. However, the sites available did not allow for long-range viewing. Also, site constraints at the dredge/fill area forced the vehicles to be located in the grass field in front of, instead of in, a tree line. This target placement was a very benign scenario from the standpoint of target detection. Within this data set, the targets are, in most

cases, readily detectable with or without the enhancements. Because of this benign test scenario, quantitative image metrics were used to extrapolate conclusions from data that can be qualitatively judged to provide enhanced detection. The following analysis takes on this format: first, a qualitative assessment of the collected data is presented; second, using image statistics, quantitative assessments are made; and finally, summary conclusions presented are based on the combined findings.

## 4.1 QUALITATIVE OBSERVATIONS

Visually apparent modulation resulting from polarization of light by target surfaces was generally of low intensity and highly dependent on illumination level. Table 4-1 presents the number of occasions under which modulation was visually discernible out of the total number of separate observations from general illumination condition and vehicle type. Each vehicle observation under starlight illumination was separated in time by one hour, and under solar or lunar illumination by source incidence angles separated by at least ten degrees. As shown, for starlight illumination viewing, modulation was not visually discernable; for lunar and solar illumination viewing, modulation was visually discernable and the number of observations increased with illumination level. In the majority of

TABLE 4-1. POLARIZATION MODULATION

| | M-113 | Jeep | M-1 | ZIL | M-2 | M-60 | Total |
|---|---|---|---|---|---|---|---|
| Starlight or Shaded from Moonlight | 0-2 | 0-2 | | 0-2 | 0-2 | 0-3 | 0-11 |
| Moonlight | 1-6 | 2-6 | | 2-6 | 1-3 | 0-5 | 6-26 |
| Twilight | 1-3 | 0-3 | 2-3 | 1-3 | | 1-3 | 5-15 |
| Daylight | 2-3 | 1-4 | 5-5 | 4-4 | 0-1 | 3-3 | 15-20 |
| Artificial | 3-3 | 0-1 | | 0-1 | | | 3-5 |
| Total | | | | | | | 29-77 |

observations, when modulation was discerned, it occurred only over limited portions of the targets.

The low ratios of detectable modulation observations versus total observations suggest, for the sensitivity of inventory night vision devices, there is little use in direct view, polarization signature enhancement modifications compared to enhanced target detection. This is not to say that the polarization signature does not exist, but rather that exploitation of this signature would require development of higher sensitivity equipment. There were two occasions where modulation due to polarization by vehicle surfaces resulted in cues that could be subjectively judged to enhance detection performance: (1) an observation of a civilian vehicle that happened to be on site during the test, and (2) an observation of the specular reflection of an artificial source (a street light) by white stripes on the M-113. These two observations will be discussed in the next section.

Target modulation resulting from spectral filtering of light reflected by target surfaces was generally of substantial visual magnitude for the observation conditions. Table 4-2 summarizes the results using spectral modulation as a function of vehicle type in the same manner as Table 4-1. Because the signal was not expected to be particularly significant under lunar and stellar illumination (see Figure 3-13), no emphasis was placed on collecting data under these conditions. A single image collected during equipment checks under starlight illumination does exhibit target modulation. In most cases, modulation was visible over large portions of the surfaces of the vehicles observed.

Although target modulation resulting from spectral filtering was easily visible in most cases, it is difficult to form any direct conclusions as to whether target detection was enhanced. The data were collected, for the most part, at short ranges under full daylight. Consequently, targets were easy to detect visually and no conclusions other than the apparent presence of the signature can be

made. Quantitative assessment of the signature provides more insight into the possible use of spectral filtering and will be discussed in the following section.

TABLE 4-2. SPECTRAL MODULATION

| | M-113 | Jeep | M-1 | ZIL | M-2 | M-60 | Total |
|---|---|---|---|---|---|---|---|
| Starlight | | | | 1-1 | | | 1-1 |
| Daylight | 3-3 | 4-4 | 4-4 | 4-4 | 1-1 | 2-2 | 18-18 |
| Total | | | | | | | 19-19 |

## 4.2 QUANTITATIVE OBSERVATIONS

A key image feature relating to target detectability is the relative prominence of the target with respect to natural background clutter. A quantitative assessment of the utility of polarization or spectral enhancements requires image metrics or measures that quantify target prominence, correlate with target detectability, and apply equally to both the enhanced and the conventional images. Several metrics are currently being used to quantify target prominence and clutter structure in imagery. A list of some of the metrics developed in the Autonomous Infrared Techniques (AIRT) Program (MDA903-84-C-0184) are given in Table 4-3. The first three relate directly to target detectability, whereas the latter four relate to how the much the background looks like a target, that is, false alarm potential.

Insight into the utility of the enhancements pursued under this program is obtained by comparing the relative prominence of the target in conventional images versus enhanced images. This comparison is best accomplished using target contrast or signal-to-noise ratio (item 1 in Table 4-3). This quantity is defined as the square of the mean target-local background contrast normalized to the local background variance. This quantity is a good measure of localized target prominence and correlates strongly with target detection performance. This metric will be referred to as local prominence. It should be

noted that the targets were generally well resolved during the data collection and, as a result, were detectable regardless of target-background contrast because features of the vehicle were identifiable. At longer ranges, particularly at ranges for which target detection is critical for RSTA applications, targets are generally not very resolved and target-background contrast is an important factor in detection performance.

TABLE 4-3. COMMONLY USED IMAGE METRICS

| Measure | Detection | Type | Comments |
|---|---|---|---|
| Signal-To-Noise Ratio (SNR) | $\frac{(\mu_T - \mu_B)^2}{\sigma_B^2}$ | Local | Target Contrast |
| Pixels on Object ($N_O$) | Number of Pixels Expected or Actually on Target at Applicable Range | Local | Resolution |
| Edge Strength Ratio (ESR) | $(\Sigma\ ES/N_O)^2/\sigma_b^2$ Where ES is a Modified Sobel Transform | Local | Structure |
| Image Signal-To-Noise Ratio (SNR) | $\frac{1}{N_c} \Sigma \frac{(\mu_T - \mu_B)^2}{\sigma_B^2}$ | Global | Clutter Contrast |
| Image Contrast Variance ($\sigma_{SNR}^2$) | Variance of Image Signal-To-Noise Ratio | Global | Clutter Contrast Variance |
| Image Edge Strength Ratio (ESR) | $\frac{1}{N_c} \Sigma \frac{(\Sigma\ ES/N_O)^2}{\sigma_B^2}$ | Global | Background Structure |
| Background Structure Variance | Variance of Image Edge Strength Ratio | Global | Background Structure Variance |

The scope of this demonstration program dictated generating statistics for a limited number of images within the collected data set. The images selected for quantitative analysis (Appendix C) are images that visually span the range of target detectability, that is, ranging from marginally detectable targets to easily detectable targets. Photographs of these digitized and analyzed images are included as an aid to the reader. For each image, the average video scene (the conventional image) is presented along with the complementary modulation component scene (the difference between the peak and minimum intensity of the modulation resulting from polar or spectral filtering). It should be noted that in the actual demonstration testing, the modulation (enhanced imagery) was, in fact, superimposed on the conventional image; it has been separated here for the purposes of presentation. A daylight color photograph (if available) of each scene is also presented.

The grey scale images presented in Appendix C are at the same magnification as the images displayed on the monitor during the test. These images, however, represent only a small portion of the total field of regard (field of view) of the sensors (i.e., a small portion of the viewed image). Detailed information on each image can be found by noting the scene number and referring to Appendix A. The "conventional" image presented for the spectrally filtered images is actually the average of the filtered (enhanced) sensor output. The conventional sensor in this case would be visual sighting of the targets. The conventional images presented in Appendix C for the spectrally filtered cases are actually averages of successive frames from the filtered sensor. However, the statistics for the conventional sensor used in the analysis of the spectrally enhanced images were extracted from images collected by the unfiltered CCD camera.

The image statistics were generated by digitizing the raw video image frames and performing computations on a personal computer. Regions within the target and surrounding backgrounds were extracted

from these images using specially developed software and the means and variances of those regions were calculated using the digital grey level of the pixels. For the statistics presented here, the background regions that were selected immediately surrounded the target and were roughly four times the area of the target. In the case of images from the dredge/fill site, the grass field in the foreground of the vehicles was omitted because its benign character yields overly optimistic variances (clutter levels) for the background.

The range of local prominence values is displayed in the first two scenes. In the first scene the target is readily detected, and in the second scene the target detectability is quite marginal. Figure C-1, which is repeated here as Figure 4-1, shows the M-113 under starlight where white stripes located on the side of the vehicle are reflecting a distant streetlight. This vehicle was easily detected when viewed through either the unmodified $L^3$ scope or the enhanced scope as a result of the modulation caused by the rotating polar filter. Figure C-2, which is repeated here as Figure 4-2, also shows the M-113, but in a different position and under lunar illumination. The vehicle was not easily detectable using the conventional scope and no polarization modulation was observed (the vehicle is slightly below and to the right of the image center, not the bright spot). Table 4-4 gives the mean grey level of the targets and backgrounds, and the standard deviation of the background for both the conventional and modulation images for both scenes. The local prominence of the targets in these images are also presented in Table 4-4. Note the radical difference in the local prominence between the two image sets. Although polarization provided a cue to test operators when the scene shown in Figure C-1 was viewed, the glint from the side of the vehicle was also sufficiently prominent to provide a cue when viewed with the unmodified sensor. It is apparent that enhanced detection performance using polar or spectral signatures requires that the local prominence of the target be enhanced.

Figure 4-1a. M-113, Scene 5, Conventional Image

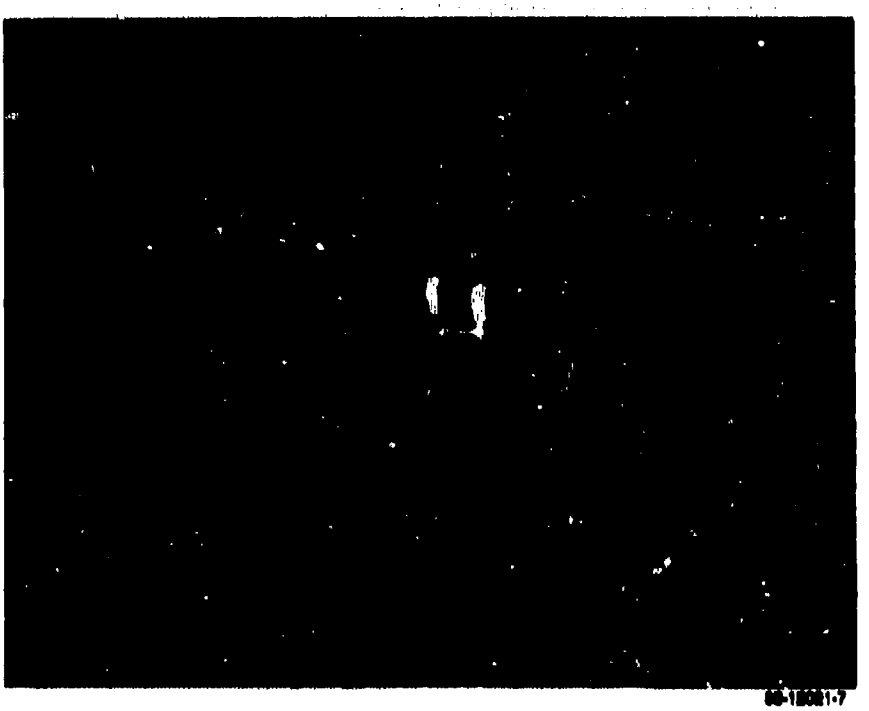

Figure 4-1b. M-113, Scene 5, Modulation Image (Polar)

89-11644-23

Figure 4-1c. M-113, Daylight Photograph (Scene 5)

89-12021-2

Figure 4-2a. M-113, Scene 3, Conventional Image

89-12021-3

Figure 4-2b. M-113, Scene 3, Modulation Image (Polar)

89-11644-9

Figure 4-2c. M-113, Daylight Photograph (Scene 3)

TABLE 4-4. STATISTICS FOR FIGURES C-1 AND C-2

| | Conventional | Modulation |
|---|---|---|
| Figure C-1 (4-1) | | |
| Target Mean | 51.9 | 15.8 |
| Background Mean | 31.8 | 0.7 |
| Background Variance ($\sigma^2$) | 10.7 | 1.2 |
| Local Prominence | 37.5 | 190.0 |
| Figure C-2 (4-2) | | |
| Target Mean | 48.7 | 2.8 |
| Background Mean | 53.1 | 2.1 |
| Background Variance ($\sigma^2$) | 51.8 | 7.3 |
| Local Prominence | 0.4 | 0.1 |

Figure 4-3 (Figure C-3) shows an image set where polarization provided a significant enhancement of detection performance by visually cueing a civilian vehicle on the site. The civilian vehicle exhibited a strong flashing cue when viewed with the modified sensor, whereas it was not readily detectable using the unmodified sensor. This difference can be seen to some degree between the average and modulation images. The local prominence value calculated for these images is 0.6 for the conventional and 22.0 for the modulation image. Obviously, a local prominence value somewhere between these two values result in improved detection performance. For more insight into the detectability of this vehicle, refer back to Figure 3-3a, which is a full field photograph of the same scene. The observer tends to readily detect the military vehicles within the scene because they are both larger and closer, but it takes a longer time to locate the automobile. Note also that this vehicle is not well resolved in the test sensor imagery. This reinforces the contention made earlier that contrast, or local prominence, is a critical parameter for detection performance at longer ranges.

89-12022-14

Figure 4-3a. Automobile, Scene 16, Conventional Image

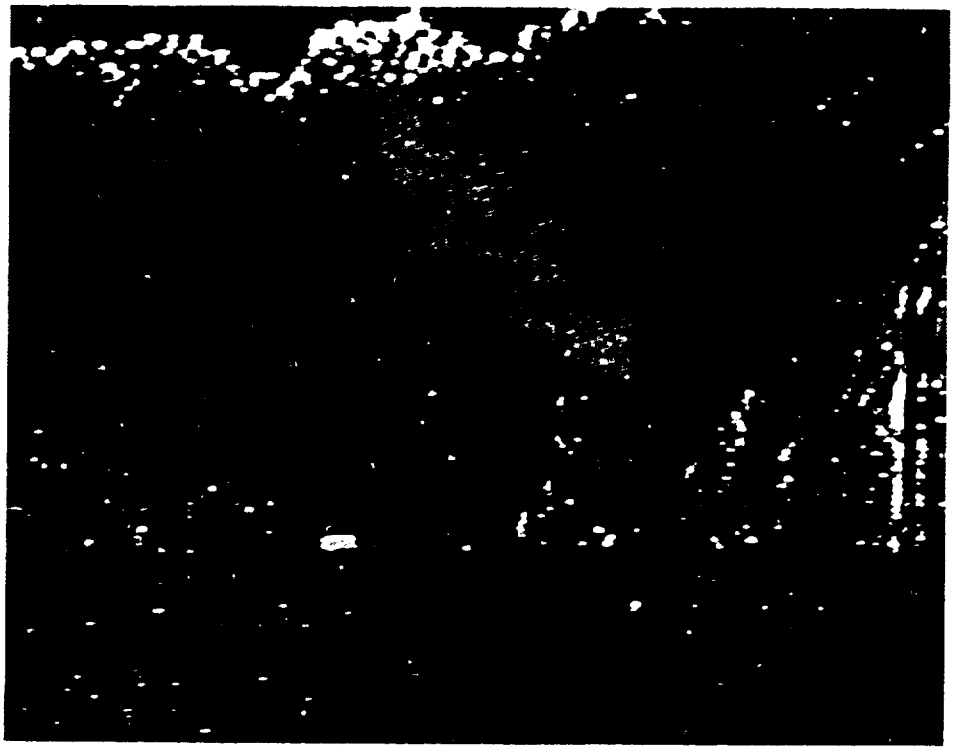

89-12022-16

Figure 4-3b. Automobile, Scene 16, Modulation Image (Polar)

A summary of the local prominence values of selected images having polar signatures is presented in Table 4-5. In this table, standard prominence and polar prominence refer to the values of the target in the conventional and polar modulation images. With the exception of the scene with the automobile and the scene where the white stripes on the side of the M-113 were visible, local prominence values for the polar signature are comparable or lower than the target prominence when viewed through the conventional sensor. With exceptions noted, one can conclude the polar signature failed to aid detection performance. Because white stripes are not usually a feature of military vehicles, and because military vehicles are not normally coated with a glossy finish like the automobile, polar enhancement does not (from this evidence) appear to improve target detection using the simple modification to existing sensors implemented in this program. To reiterate, polar signatures were visible only over relatively small portions of the target surface and, consequently, may subtend an angle smaller than the angular resolution of a sensor at longer ranges.

TABLE 4-5. POLAR ENHANCEMENT LOCAL PROMINENCE SUMMARY

| | Figure Number | Standard Prominence | Polar Prominence | Comments |
|---|---|---|---|---|
| Moon Illuminated | C-2 | 0.4 | 0.1 | Modulation Scenes Not Visible |
| | C-5 | 9.3 | 3.4 | |
| | C-6 | 2.7 | 0.9 | |
| | C-7 | 3.6 | 3.7 | O.D. Paint |
| | C-10 | 2.3 | 3.5 | |
| Twilight | C-8 | 5.2 | 0.23 | Modulation Scenes Barely Visible |
| Daylight Scenes | C-3 | 0.6 | 22.0 | Civilian Car |
| | C-9 | 2.3 | 2.3 | Rear of M-1 |
| | C-11 | 5.7 | 18.5 | Front of M-1 |
| Artificial Illumination | C-1 | 37.5 | 190.0 | White Stripes |
| | C-4 | 1.1 | 15.7 | White Stripes |
| | C-7 | 3.6 | 55.9 | White Stripes |

Figure 4-4 (Figure C-13) illustrates results typical of the spectral modulation signature of vehicles. In the modulation image, it appears that the cluttered structure of the wooded background has been almost entirely eliminated. Also, the outline of the vehicles is apparent and the modulation was visible over most of the vehicle surfaces (including some degree of modulation over the camouflage netting).

The reason for the apparent modulation of the grass in the foreground of the vehicles in Figure C-13 is not known. However, it has been noted that this effect occurred only in areas near the line of sight of the sensor rather than to the left and right portions of the image. This was true regardless of the direction the sensor was pointed, that is, the effect seemed to follow the sensor. Because of this, and because the sensor operation was detrimentally affected by direct sky radiation as was mentioned earlier, one explanation which has been forwarded is that this effect was caused by sensor internal scattering of sky radiation from outside of the field of view. Another possibility is that the grass exhibited a greater specular component as opposed to the more diffusely illuminated woods. It is interesting to note that although the effect is quite apparent in the modulation images presented here, it was not noticed by test personnel while collecting the data.

A summary of the local prominence values of the images having spectral signatures is presented in Table 4-6. In this table, standard prominence refers to the prominence of targets when viewed with an unfiltered CCD camera, and spectral prominence refers to the prominence values of the target in the spectral modulation images. Note that not only are spectral prominence values high, but that the visual prominence (contrast) is modest as expected of military vehicles and camouflage netting. This indicates that the spectral comparison technique used here offers a potentially useful signature;

however, a more robust data collection would be required to firmly establish the use of spectral filtering. Also, the sensor implementation used had defects (as noted above and in Section 3.3) and would need modifications for any further effort.

89-11645-8

Figure 4-3c. Automobile, Daylight Photograph

89-12022-4

Figure 4-4a. M-1 and ZIL, Scene 38, Image Average

89-12022-6

Figure 4-4b. M-1 and ZIL, Scene 38, Modulation Image (Spectral)

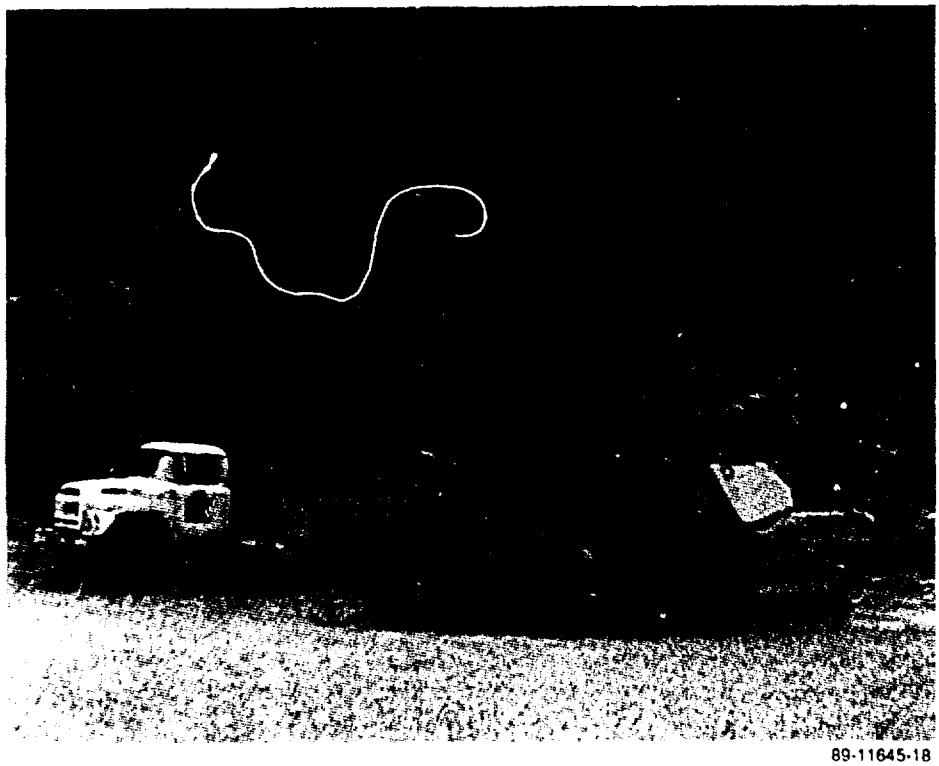

89-11645-18

Figure 4-4c. M-1 and ZIL, Daylight Photograph (Note Camouflage Net)

TABLE 4-6. SPECTRAL ENHANCEMENT LOCAL PROMINENCE SUMMARY

| | Figure Number | Standard Prominence | Spectral Prominence | Comments/ Target |
|---|---|---|---|---|
| Daylight Scenes | C-12 | 0.4 | 23.0 | M-1 tank |
| | C-12 | 3.0 | 59.3 | ZIL |
| | C-13 | 1.6 | 88.4 | M-1 tank |
| | C-13 | 0.3 | 79.2 | ZIL |
| | C-13 | 0.0 | 34.8 | Camouflage |
| | C-14 | 2.0 | 13.0 | Jeep |
| | C-16 | 1.4 | 6.8 | M-113 |
| Starlight Scene | C-15 | 0.5 | 4.4 | ZIL |

## 4.3 CONCLUSIONS

The purpose of this section is to offer summary conclusions from this analysis. The conclusions are presented at a level consistent with the program objective: to examine and evaluate specific physical phenomena and assess the possibility of exploiting the phenomena to enhance the performance of existing man-in-the-loop electro-optical RSTA systems. A secondary objective was to suggest and demonstrate device modifications that could provide (1) significant performance enhancements or new capabilities at low cost, or (2) provide comparable performance at a reduced cost. Following are the conclusions with respect to the polarization and spectral signatures.

### Spectral Filtering

Within the data set of this demonstration, the modulation produced by spectral filtering clearly enhanced detection performance. The enhancement was particularly noteworthy because the demonstration equipment was not optimized for the exploitation of this signature. Further investigation of this near infrared phenomenology for improved detection by direct view system is strongly recommended. However, to conduct a detailed investigation of this signature, the demonstration hardware used in this program should be modified to accommodate the indepth trade-offs necessary to optimize the enhancement. Therefore, the recommendations are (1) modify the existing demonstration

equipment for the exclusive investigation of spectral filtering, (2) further data collection to validate the utility of the signature over a broad range of environmental and target conditions, and (3) develop a low cost implementation concept which optimizes the exploitation of this signature.

Polarization

As predicted, polarization target signatures were observed under a variety of illumination conditions; however, due to the sensitivity of the $L^3$ scopes used, generally the signatures were of low magnitude and appeared to have little operational utility. As the $L^3$ scopes used represent state-of-the-art, high quantum efficiency technology, there is little likelihood of near term exploitation of this enhancement. It is important to note that the conclusion drawn here applies only to direct view, visual and $L^3$ systems. The utility of polarization signatures in active systems has been demonstrated by the WES REMIDS sensor, and the utility of polarization is being studied by ERIM and others for passive sensors operation in other spectral regions.

## 4.4 RECOMMENDATIONS FOR PHASE II

Based on the above conclusions, further investigation of the utility of the near IR spectral characteristics of targets for performance enhancement of direct view RSTA systems is recommended. A follow-on program focused on exploiting near IR spectral signatures (with an expanded and specially tailored test program) could be conducted for nominally the same level of effort as the EO Target Enhancement Program. Ideally, such a program would take one year to allow testing in all four seasons. An analysis of the spectral signatures would be performed to optimize the filter band centers and bandwidths. Selected bands would be tested to validate performance predictions.

## 5.0 REFERENCES


1. V. Leeman, D. Earing, R. Vincent, and S. Ladd, The NASA Earth Resources Spectral Information System: A Data Compilation, Report No. NASA CR-31650-24-T, Institute of Science and Technology, The University of Michigan, Ann Arbor, May 1971.

2. IST Staff, Target Signature Analysis Center: Data Compilation, Eleventh Supplement, Vol. II, Report No. AFAL-TR-72-226, Target Signature Analysis Center, Willow Run Laboratories, The University of Michigan, Ann Arbor, October 1972.

3. J. M. Brawn and P.C. Driver, A Study of Target Detection Enhancement at Low Light Levels using Polarization and Luminance Discrimination Techniques, Report No. IPD-2768, Electro-Optical Branch, Aviation Ordinance Department, Naval Weapons Center, China Lake, California, August 1967.

4. D. Falkner, R. Horvath, J.P. Ulrich and E. Work, Spectral and Polarization Characteristics of Selected Targets and Backgrounds: Instrumentation and Measured Results (3.3 to 14.0 microns), Report No. AFAL-TR-71-199, Willow Run Laboratories, Institute of Science and Technology, The University of Michigan, Ann Arbor, August 1971.

5. Target and Background Characteristics: Analysis and Applications, Technical Report AFAL-TR-71-239, Willow Run Laboratories, Institute of Science and Technology, The University of Michigan, Ann Arbor, October 1971.

6. J.L. Johnson, Infrared Polarization Signature Feasibility Tests, Report No. TR-EO-74-1, Chrysler Corporation Space Division, New Orleans, Louisiana, May 1974.

7. Nautical Almanac Office, The American Ephemeris and Nautical Almanac, United States Naval Observatory, pp. 468-485, 1966.

8. L. M. Biberman and S. Nudelman, Photoelectronic Imaging Devices, Vol. I, Plenum Press, New York, NY, 1971.

# APPENDIX A. SUMMARY OF RAW DATA

The following summarizes the raw data, collected on video tape, during the demonstration test September 18 through 22, 1989. Each subsection describes a contiguous segment of the video tape collected. Included are the date and time at which recording began, the configuration of sensors and filters used, the location from which observations were made, the vehicles observed, and the approximate bearing and range to each. Also included are general observations noted during each data collection. The solar and lunar coordinates and scene illumination (where given) are calculated values included for reference.

Scene 1

Date: 18 September 1989
Time: 2300 hrs
Sensor Used: Spectral filters alternating at 3 Hz in front of L3 scope. Output monitored using CCD camera.

Observation Point: OP4 (Dredge/Fill Site)
Sun Elevation (deg): N/A Azimuth:
Moon Elevation (deg): 22.2 Azimuth: 80.3
Lunar Phase (%): 73
Estimated In-Band Irradiance (μW/cm^2): 321

| Vehicle Sites Viewed | Approximate Line of Sight and Range | |
|---|---|---|
| VS8 (Soviet ZIL) | 115° | 160 yds |

Additional Comments

A 10% transmission neutral density filter was used over the 0.85 μm spectral filter instead of the 30% transmission filter. Modulation of background results from incorrect transmission.

Sky is clear.

Scene 2

Date: 19 September 1989
Time: 0012 hrs
Sensor Used: Dichroic polarizer cycling at 5 Hz in front of L3 scope. Output monitored using CCD camera.

Observation Point: OP5 (Dredge/Fill Site)
Sun Elevation (deg): N/A Azimuth:
Moon Elevation (deg): 37.0 Azimuth: 88.6
Lunar Phase (%): 72
Estimated In-Band Irradiance ($\mu$W/cm^2): 357

| Vehicle Sites Viewed | Approximate Line of Sight and Range | |
|---|---|---|
| VS1 (M-113 APC) | 246° | 90 yds |
| VS2 (M-60 Tank) | 196° | 110 yds |
| VS8 (Soviet ZIL) | | 170 yds |
| VS9 (M-151 Jeep) | | 210 yds |

Additional Comments

Line of sight starts on VS9 then pans to VS1. No polarization noted. M-60 is shaded from moonlight by trees. Sky is clear.

Scene 3

Date: 19 September 1989
Time: 0017 hrs
Sensor Used: Dichroic polarizer cycling at 5 Hz in front of L3 scope. Output monitored using CCD camera.

Observation Point: OP5 (Dredge/Fill Site)
Sun Elevation (deg): N/A Azimuth:
Moon Elevation (deg): 38.0 Azimuth: 89.2
Lunar Phase (%): 72
Estimated In-Band Irradiance ($\mu$W/cm^2): 359

| Vehicle Sites Viewed | Approximate Line of Sight and Range | |
|---|---|---|
| VS1 (M-113 APC) | 246° | 90 yds |
| VS2 (M-60 Tank) | 196° | 110 yds |
| VS8 (Soviet ZIL) | | 170 yds |
| VS9 (M-151 Jeep) | | 210 yds |

Additional Comments

Line of sight starts on VS1, pans to VS2 and then to VS8 and VS9. No polarization noted. M-60 is shaded from moonlight by trees.

Sky is clear.

Scene 4

Date: 19 September 1989
Time: 2057 hrs
Sensor Used: Dichroic polarizer cycling at 5 Hz in front of L3 scope. Output monitored using CCD camera.

Observation Point: OP3 (Dredge/Fill Site)
Sun Elevation (deg): N/A Azimuth:
Moon Elevation (deg): N/A Azimuth:
Lunar Phase (%): N/A
Estimated In-Band Irradiance ($\mu$W/cm^2): N/A

| Vehicle Sites Viewed | Approximate Line of Sight and Range | |
|---|---|---|
| VS3 (M-60 Tank) | 218° | 110 yds |
| VS4 (M-113 APC) | 206° | 90 yds |
| VS5 (M-151 Jeep) | 191° | 80 yds |
| VS7 (Soviet ZIL) | 171° | 100 yds |

Additional Comments

Line of sight pans from VS7 through all vehicles to VS3 and returns to VS4.

Dominant polar modulation from M-113 APC. Presumed to be from specular reflection of distant outside light from neoprene tread skirt and small glossy white tabs on front and aft of vehicle side. No polarization noted on other vehicles.

Sky is clear.

## Scene 5

Date: 19 September 1989
Time: 2111 hrs
Sensor Used: Dichroic polarizer cycling at 2.5 Hz in front of L3 scope. Output monitored using CCD camera.

Observation Point: OP3 (Dredge/Fill Site)
Sun Elevation (deg): N/A Azimuth:
Moon Elevation (deg): N/A Azimuth:
Lunar Phase: N/A
Estimated In-Band Irradiance (μW/cm^2): N/A

| Vehicle Sites Viewed | Approximate Line of Sight and Range | |
|---|---|---|
| VS3 (M-60 Tank) | 218° | 110 yds |
| VS4 (M-113 APC) | 206° | 90 yds |
| VS5 (M-151 Jeep) | 191° | 80 yds |
| VS7 (Soviet ZIL) | 171° | 100 yds |

Additional Comments

Line of sight pans from VS7 through all vehicles to VS3 and returns. Pans again to VS4.

Dominant polar modulation from M-113 APC. Presumed to be from specular reflection of distant outside light from neoprene tread skirt and small glossy white tabs on front and aft of vehicle side. No polarization noted on other vehicles.

Sky is clear.

## Scene 6

Date: 19 September 1989
Time: 2156 hrs
Sensor Used: Dichroic polarizer cycling at 2.5 Hz in front of L3 scope. Output monitored using CCD camera.

Observation Point: OP6 (Dredge/Fill Site)
Sun Elevation (deg): N/A Azimuth:
Moon Elevation (deg): 1.0 Azimuth: 62.3
Lunar Phase (%): 65
Estimated In-Band Irradiance (μW/cm^2): 22

| Vehicle Sites Viewed | Approximate Line of Sight | and Range |
|---|---|---|
| VS3 (M-60 Tank) | | 400 yds |
| VS4 (M-113 APC) | 256° | 360 yds |
| VS5 (M-151 Jeep) | | 340 yds |
| VS7 (Soviet ZIL) | 251° | 320 yds |

Additional Comments

Line of sight pans from right through all vehicles and returns to position where all vehicles are in the field of view. No polarization noted. Moon not sufficiently elevated to illuminate targets.

Sky is clear.

## Scene 7

Date: 19 September 1989
Time: 2223 hrs
Sensor Used: Dichroic polarizer cycling at 2.5 Hz in front of L3 scope. Output monitored using CCD camera.

Observation Point: OP7 (Poor/House Site)
Sun Elevation (deg): N/A Azimuth:
Moon Elevation (deg): 6.0 Azimuth: 65.5
Lunar Phase (%): 65
Estimated In-Band Irradiance ($\mu$W/cm^2): 104

| Vehicle Sites Viewed | Approximate Line of Sight and Range | |
|---|---|---|
| VS12 (M-2 Bradley) | 66° | 150 yds |

Additional Comments

Line of sight pans from right onto VS12. Imagery extremely dark and vehicle hardly discernable. No polarization noted. Target shaded from moonlight.

Sky is clear.

Scene 8

Date: 19 September 1989
Time: 2307 hrs
Sensor Used: Dichroic polarizer cycling at 2.5 Hz in front of L3 scope. Output monitored using CCD camera.

Observation Point: OP6 (Dredge/Fill Site)
Sun Elevation (deg): N/A Azimuth:
Moon Elevation (deg): 14.3 Azimuth: 70.4
Lunar Phase (%): 65
Estimated In-Band Irradiance ($\mu W/cm^2$): 231

| Vehicle Sites Viewed | Approximate Line of Sight and Range | |
|---|---|---|
| VS3 (M-60 Tank) | | 400 yds |
| VS4 (M-113 APC) | 256° | 360 yds |
| VS5 (M-151 Jeep) | | 340 yds |
| VS7 (Soviet ZIL) | 251° | 320 yds |

Additional Comments

Line of sight stares at all vehicles. No polarization noted.

Sky is clear.

Scene 7

Date: 20 September 1989
Time: 0014 hrs
Sensor Used: Dichroic polarizer cycling at 2.5 Hz in front of L3 scope. Output monitored using CCD camera.

Observation Point: OP3 (Dredge/Fill Site)
Sun Elevation (deg): N/A Azimuth:
Moon Elevation (deg): 27.5 Azimuth: 77.4
Lunar Phase (%): 65
Estimated In-Band Irradiance ($\mu$W/cm^2): 303

| Vehicle Sites Viewed | Approximate Line of Sight and Range | |
|---|---|---|
| VS3 (M-60 Tank) | 218° | 110 yds |
| VS4 (M-113 APC) | 206° | 90 yds |
| VS5 (M-151 Jeep) | 191° | 80 yds |
| VS7 (Soviet ZIL) | 171° | 100 yds |

Additional Comments

Line of sight pans from left through all vehicles and returns, pausing on each vehicle.

The M-113, jeep and ZIL exhibit polarization. Polarization on ZIL and jeep appear to be caused by specular reflection of moonlight whereas polarization on M-113 appears to be specular reflection of distant outside light as in Scene 5.

Sky is clear.

Scene 10

Date: 20 September 1989
Time: 0021 hrs
Sensor Used: Dichroic polarizer cycling at 2.5 Hz in front of L3 scope. Output monitored using CCD camera.

Observation Point: OP3 (Dredge/Fill Site)
Sun Elevation (deg): N/A Azimuth:
Moon Elevation (deg): 28.9 Azimuth: 78.1
Lunar Phase (%): 65
Estimated In-Band Irradiance (μW/cm^2): 306

| Vehicle Sites Viewed | Approximate Line of Sight and Range | |
|---|---|---|
| VS3 (M-60 Tank) | 218° | 110 yds |
| VS4 (M-113 APC) | 206° | 90 yds |
| VS5 (M-151 Jeep) | 191° | 80 yds |
| VS7 (Soviet ZIL) | 171° | 100 yds |

Additional Comments

Line of sight tracking man walking down road. Movement provides cue. Vehicles exhibit polarization as in Scene 9.

Sky is clear.

Scene 11

Date: 20 September 1989
Time: 0055 hrs
Sensor Used: Dichroic polarizer cycling at 2.5 Hz in front of L3 scope. Output monitored using CCD camera.

Observation Point: OP6 (Dredge/Fill Site)
Sun Elevation (deg): N/A Azimuth:
Moon Elevation (deg): 35.8 Azimuth: 81.6
Lunar Phase (%): 65
Estimated In-Band Irradiance ($\mu$W/cm^2): 319

| Vehicle Sites Viewed | Approximate Line of Sight and Range | |
|---|---|---|
| VS3 (M-60 Tank) | | 400 yds |
| VS4 (M-113 APC) | 256° | 360 yds |
| VS5 (M-151 Jeep) | | 340 yds |
| VS7 (Soviet ZIL) | 251° | 320 yds |

Additional Comments

Line of sight stares at all vehicles. No polarization noted.

Sky is clear.

Scene 12

Date: 19 September 1989
Time: 0112 hrs
Sensor Used: Dichroic polarizer cycling at 2.5 Hz in front of L3 scope. Output monitored using CCD camera.

Observation Point: OP7 (Poor House Site)
Sun Elevation (deg): N/A Azimuth:
Moon Elevation (deg): 39.3 Azimuth: 83.4
Lunar Phase (%): 64
Estimated In-Band Irradiance (μW/cm^2): 320

| Vehicle Sites Viewed | Approximate Line of Sight and Range | |
|---|---|---|
| VS12 (M-2 Bradley) | 66° | 150 yds |

Additional Comments

Line of sight stares at vehicle. No polarization noted. Target shaded from moonlight. Vegetation in foreground exhibits polarization and is attributed to dew forming on the leaves.

Sky is clear.

Scene 13

Date: 20 September 1989
Time: 0250 hrs
Sensor Used: Dichroic polarizer cycling at 2.5 Hz in front of L3 scope. Output monitored using CCD camera.

Observation Point: OP3 (Dredge/Fill Site)
Sun Elevation (deg): N/A Azimuth:
Moon Elevation (deg): 59.4 Azimuth: 95.5
Lunar Phase (%): 64
Estimated In-Band Irradiance (μW/cm^2): 341

| Vehicle Sites Viewed | Approximate Line of Sight and Range | |
|---|---|---|
| VS3 (M-60 Tank) | 218° | 110 yds |
| VS4 (M-113 APC) | 206° | 90 yds |
| VS5 (M-151 Jeep) | 191° | 80 yds |
| VS7 (Soviet ZIL) | 171° | 100 yds |

Additional Comments

Line of sight pans from left through all vehicles and returns, pausing on each vehicle.

The M-113, jeep and ZIL exhibit polarization. Polarization on ZIL and jeep appear to be caused by specular reflection of moonlight whereas polarization on side of M-113 appears to be specular reflection of distant outside light as in Scene 5. Polarization on front of M-113 now apparent and appears to be a specular reflection of moonlight.

Vehicles in scene are wet from dew.

Sky is clear.

Scene 14

Date: 20 September 1989
Time: 0302 hrs
Sensor Used: Dichroic polarizer cycling at 2.5 Hz in front of L3 scope. Output monitored using CCD camera.

Observation Point: OP6 (Dredge/Fill Site)
Sun Elevation (deg): N/A Azimuth:
Moon Elevation (deg): 61.9 Azimuth: 97.5
Lunar Phase (%): 64
Estimated In-Band Irradiance ($\mu$W/cm^2): 343

| Vehicle Sites Viewed | Approximate Line of Sight and Range | |
|---|---|---|
| VS3 (M-60 Tank) | | 400 yds |
| VS4 (M-113 APC) | 256° | 360 yds |
| VS5 (M-151 Jeep) | | 340 yds |
| VS7 (Soviet ZIL) | 251° | 320 yds |

Additional Comments

Line of sight stares at all vehicles. No polarization noted.

Sky is clear.

Scene 15

Date: 20 September 1989
Time: 0316 hrs
Sensor Used: Dichroic polarizer cycling at 2.5 Hz in front of L3 scope. Output monitored using CCD camera.

Observation Point: OP7 (Poor House Site)
Sun Elevation (deg): N/A Azimuth:
Moon Elevation (deg): 64.8 Azimuth: 100.1
Lunar Phase (%): 64
Estimated In-Band Irradiance (μW/cm^2): 344

| Vehicle Sites Viewed | Approximate Line of Sight and Range | |
|---|---|---|
| VS12 (M-2 Bradley) | 66° | 150 yds |

Additional Comments

Line of sight pans from right onto VS12. Vehicle exhibits polarization which is attributed to specular reflection of moonlight.

Sky is clear.

Scene 16

Date: 21 September 1989
Time: 1352 hrs
Sensor Used: Dichroic polarizer cycling at 2.5 Hz in front of CCD camera.

Observation Point: OP6 (Dredge/Fill Site)
Sun Elevation (deg): 55.5 Azimuth: 205.0
Moon Elevation (deg): N/A Azimuth:
Lunar Phase (%): N/A
Estimated In-Band Irradiance ($\mu$W/cm^2):

| Vehicle Sites Viewed | Approximate Line of Sight and Range | |
|---|---|---|
| VS3 (M-60 Tank) | | 400 yds |
| VS4 (M-113 APC) | 256° | 360 yds |
| VS5 (M-151 Jeep) | | 340 yds |
| VS7 (Soviet ZIL) | 251° | 320 yds |
| VS1 (Civilian Vehicle) | | 500 yds |

Additional Comments

Line of sight pans from right through all vehicles and returns to car and zooms in.

Car flashes distinctively. All vehicles exhibit polarization.

Sky is clear.

Scene 17

Date: 21 September 1989
Time: 1434 hrs
Sensor Used: Calcite polarizer cycling at 2.5 Hz in front of CCD camera.

Observation Point: OP7 (Poor House Site)
Sun Elevation (deg): 50.7 Azimuth: 220.6
Moon Elevation (deg): N/A Azimuth:
Lunar Phase (%): N/A
Estimated In-Band Irradiance (μW/cm^2):

| Vehicle Sites Viewed | Approximate Line of Sight and Range | |
|---|---|---|
| VS12 (M-2 Bradley) | 66° | 150 yds |

Additional Comments

Line of sight stares at vehicle. Vehicle partially camouflaged by tree branches. Vehicle exhibits little or no polarization.

Sky is clear.

Scene 18

Date: 21 September 1989
Time: 1437 hrs
Sensor Used: Dichroic polarizer cycling at 2.5 Hz in front of CCD camera.

Observation Point: OP7 (Poor House Site)
Sun Elevation (deg): 50.3 Azimuth: 221.6
Moon Elevation (deg): N/A Azimuth:
Lunar Phase (%): N/A
Estimated In-Band Irradiance (μW/cm^2):

| Vehicle Sites Viewed | Approximate Line of Sight and Range | |
|---|---|---|
| VS12 (M-2 Bradley) | 66° | 150 yds |

Additional Comments

Line of sight stares at vehicle. Little or no polarization noted.

Sky is clear.

Scene 19

Date: 21 September 1989
Time: 1446 hrs
Sensor Used: Dichroic polarizer cycling at 2.5 Hz in front of CCD camera.

Observation Point: OP7 (Poor House Site)
Sun Elevation (deg): 50.0 Azimuth: 224.4
Moon Elevation (deg): N/A Azimuth:
Lunar Phase (%): N/A
Estimated In-Band Irradiance (μW/cm^2):

| Vehicle Sites Viewed | Approximate Line of Sight and Range | |
|---|---|---|
| VS12 (M-2 Bradley) | 66° | 150 yds |

Additional Comments

Line of sight stares at vehicle. Little or no polarization noted.

Sky is clear.

Scene 20

Date: 21 September 1989
Time: 1513 hrs
Sensor Used: Dichroic polarizer cycling at 2.5 Hz in front of CCD camera.

Observation Point: OP1 (Dredge/Fill Site)
Sun Elevation (deg): 44.7 Azimuth: 232.1
Moon Elevation (deg): N/A Azimuth:
Lunar Phase (%): N/A
Estimated In-Band Irradiance (μW/cm^2):

| Vehicle Sites Viewed | Approximate Line of Sight and Range | |
|---|---|---|
| VS3 (M-60 Tank) | | 360 yds |
| VS4 (M-113 APC) | | 340 yds |
| VS5 (M-151 Jeep) | | 330 yds |
| VS6 (M-1 Tank) | 211° | 330 yds |
| VS7 (Soviet ZIL) | | 330 yds |

Additional Comments

Line of sight starts on VS6 and pans to each vehicle. Polarization quite apparent on M-1 and the outline of the M-60. The ZIL also exhibits polarization.

Sky is clear.

Scene 21

Date: 21 September 1989
Time: 1523 hrs
Sensor Used: Dichroic polarizer cycling at 2.5 Hz in front of CCD camera.

Observation Point: OP1 (Dredge/Fill Site)
Sun Elevation (deg): 43.0 Azimuth: 234.6
Moon Elevation (deg): N/A Azimuth:
Lunar Phase (%): N/A
Estimated In-Band Irradiance (μW/cm^2):

| Vehicle Sites Viewed | Approximate Line of Sight and Range | |
|---|---|---|
| VS3 (M-60 Tank) | | 360 yds |
| VS4 (M-113 APC) | | 340 yds |
| VS5 (M-151 Jeep) | | 330 yds |
| VS6 (M-1 Tank) | 211° | 330 yds |
| VS7 (Soviet ZIL) | | 330 yds |

Additional Comments

Line of sight starts on VS6 and pans to each vehicle. Polarization quite apparent on M-1 and the outline of the M-60. The ZIL and M-113 also exhibit polarization.

Sky is clear.

Scene 22

Date: 21 September 1989
Time: 1529 hrs
Sensor Used: Dichroic polarizer cycling at 2.5 Hz in front of CCD camera.

Observation Point: OP1 (Dredge/Fill Site)
Sun Elevation (deg): 42.0 Azimuth: 236.1
Moon Elevation (deg): N/A Azimuth:
Lunar Phase (%): N/A
Estimated In-Band Irradiance ($\mu$W/cm^2):

| Vehicle Sites Viewed | Approximate Line of Sight and Range |
|---|---|
| VS3 (M-60 Tank) | 360 yds |
| VS4 (M-113 APC) | 340 yds |

Additional Comments

Line of sight on VS3. Man walking down road. Polarization apparent on both M-60 and M-113.

Sky is clear.

Scene 23

Date: 21 September 1989
Time: 1530 hrs
Sensor Used: Dichroic polarizer cycling at 2.5 Hz in front of CCD camera.

Observation Point: OP1 (Dredge/Fill Site)
Sun Elevation (deg): 42.0 Azimuth: 236.1
Moon Elevation (deg): N/A Azimuth:
Lunar Phase (%): N/A
Estimated In-Band Irradiance ($\mu$W/cm^2):

| Vehicle Sites Viewed | Approximate Line of Sight and Range |
|---|---|
| VS3 (M-60 Tank) | 360 yds |

Additional Comments

Line of sight on VS3. Outline of M-60 highly polarized. Sky is clear.

Scene 24

Date: 21 September 1989
Time: 1547 hrs
Sensor Used: Dichroic polarizer cycling at 2.5 Hz in front of CCD camera.

Observation Point: OP1 (Dredge/Fill Site)
Sun Elevation (deg): 38.7 Azimuth: 240.2
Moon Elevation (deg): N/A Azimuth:
Lunar Phase (%): N/A
Estimated In-Band Irradiance ($\mu W/cm^2$):

| Vehicle Sites Viewed | Approximate Line of Sight and Range | |
|---|---|---|
| VS5 (M-151 Jeep) | | 330 yds |
| VS6 (M-1 Tank) | 211° | 330 yds |
| VS7 (Soviet ZIL) | | 330 yds |
| M-15 Anti Tank Mines (3) | | 10 yds |

Additional Comments

Line of sight towards VS6. Polarization visible on mines in foreground and vehicles to the rear. Image zooms in on the mines.

Sky is clear.

Scene 25

Date: 21 September 1989
Time: 1947 hrs
Sensor Used: Dichroic polarizer cycling at 2.5 Hz in front of L3 scope. Output monitored using CCD camera.

Observation Point: OP3 (Dredge/Fill Site)
Sun Elevation (deg): N/A Azimuth:
Moon Elevation (deg): N/A Azimuth:
Lunar Phase (%): N/A
Estimated In-Band Irradiance ($\mu W/cm^2$):

| Vehicle Sites Viewed | Approximate Line of Sight and Range | |
|---|---|---|
| VS3 (M-60 Tank) | 218° | 110 yds |
| VS4 (M-113 APC) | 206° | 90 yds |
| VS5 (M-151 Jeep) | 191° | 80 yds |
| VS6 (M-1 Tank) | 181° | 80 yds |
| VS7 (Soviet ZIL) | 171° | 100 yds |

Additional Comments

Line of starts on VS6, pans to VS4 and returns. Slight polarization visible on M-1.

Sky is clear. Twilight illumination.

Scene 26

Date: 22 September 1989
Time: 0532 hrs
Sensor Used: Dichroic polarizer cycling at 2.5 Hz in front of L3 scope. Output monitored using CCD camera.

Observation Point: OP6 (Dredge/ Fill Site)
Sun Elevation (deg): N/A Azimuth:
Moon Elevation (deg): 68.3 Azimuth: 97.1
Lunar Phase (%): 48
Estimated In-Band Irradiance (μW/cm^2): 259

| Vehicle Sites Viewed | Approximate Line of Sight and Range | |
|---|---|---|
| VS3 (M-60 Tank) | | 400 yds |
| VS4 (M-113 APC) | 256° | 360 yds |
| VS5 (M-151 Jeep) | | 340 yds |
| VS6 (M-1 Tank) | | 330 yds |
| VS7 (Soviet ZIL) | 251° | 320 yds |

Additional Comments

Line of sight toward VS6. Ground fog obscures all vehicles.

Sky is clear.

Scene 27

Date: 22 September 1989
Time: 0551 hrs
Sensor Used: Dichroic polarizer cycling at 2.5 Hz in front of L3 scope. Output monitored using CCD camera.

Observation Point: OP7 (Poor House Site)
Sun Elevation (deg): N/A Azimuth:
Moon Elevation (deg): 72.1 Azimuth: 101.3
Lunar Phase (%): 48
Estimated In-Band Irradiance ($\mu$W/cm^2): 260

| Vehicle Sites Viewed | Approximate Line of Sight and Range | |
|---|---|---|
| VS12 (M-2 Bradley) | 66° | 150 yds |

Additional Comments

Line of sight on VS12. No polarization noted.
Sky is clear.

Scene 28

Date: 22 September 1989
Time: 0555 hrs
Sensor Used: Dichroic polarizer cycling at 2.5 Hz in front of L3 scope. Output monitored using CCD camera.

Observation Point: OP7 (Poor House Site)
Sun Elevation (deg): N/A Azimuth:
Moon Elevation (deg): 72.9 Azimuth: 102.3
Lunar Phase (%): 48
Estimated In-Band Irradiance (μW/cm^2): 261

| Vehicle Sites Viewed | Approximate Line of Sight and Range | |
|---|---|---|
| VS12 (M-2 Bradley) | 66° | 150 yds |

Additional Comments

Line of sight on VS12. No polarization noted.
Sky is clear.

Scene 29

Date: 22 September 1989
Time: 0625 hrs
Sensor Used: Dichroic polarizer cycling at 2.5 Hz in front of L3 scope. Output monitored using CCD camera.

Observation Point: OP7 (Poor House Site)
Sun Elevation (deg): N/A Azimuth:
Moon Elevation (deg): 78.8 Azimuth: 113.9
Lunar Phase (%): 48
Estimated In-Band Irradiance ($\mu$W/cm^2): 263

| Vehicle Sites Viewed | Approximate Line of Sight and Range | |
|---|---|---|
| VS12 (M-2 Bradley) | 66° | 150 yds |

Additional Comments

Line of sight on VS12. No polarization noted.
Sky is clear.

Scene 30

Date: 22 September 1989
Time: 0646 hrs
Sensor Used: Dichroic polarizer cycling at 2.5 Hz in front of CCD camera.

Observation Point: OP1 (Dredge/Fill Site)
Sun Elevation (deg): N/A Azimuth:
Moon Elevation (deg): 82.5 Azimuth: 130.8
Lunar Phase (%): 48
Estimated In-Band Irradiance ($\mu$W/cm^2):

| Vehicle Sites Viewed | Approximate Line of Sight and Range | |
|---|---|---|
| VS5 (M-151 Jeep) | | 330 yds |
| VS6 (M-1 Tank) | 211° | 330 yds |
| VS7 (Soviet ZIL) | | 330 yds |

Additional Comments

Line of sight on VS6. Polar filter both rotating and stationary. Heavy ground fog. No polarization noted on vehicles. Scene illuminated by twilight.

Sky is clear.

Scene 31

Date: 22 September 1989
Time: 0655 hrs
Sensor Used: Dichroic polarizer cycling at 2.5 Hz in front of CCD camera.

Observation Point: OP1 (Dredge/Fill Site)
Sun Elevation (deg): N/A Azimuth:
Moon Elevation (deg): 83.7 Azimuth: 143.3
Lunar Phase (%): 48
Estimated In-Band Irradiance ($\mu$W/cm^2):

| Vehicle Sites Viewed | Approximate Line of Sight and Range | |
|---|---|---|
| VS3 (M-60 Tank) | | 360 yds |
| VS4 (M-113 APC) | | 340 yds |
| VS5 (M-151 Jeep) | | 330 yds |
| VS6 (M-1 Tank) | 211° | 330 yds |
| VS7 (Soviet ZIL) | | 330 yds |

Additional Comments

Line of sight towards VS6 then pans to M-113 and M-60. The M-1, ZIL, M-113 and M-60 exhibit polarization. Scene illuminated by twilight.

Sky is partially overcast.

Scene 32

Date: 22 September 1989
Time: 0701 hrs
Sensor Used: Dichroic polarizer cycling at 2.5 Hz in front of CCD camera.

Observation Point: OP1 (Dredge/Fill Site)
Sun Elevation (deg): 1.1 Azimuth: 90.4
Moon Elevation (deg): 84.4 Azimuth: 154.2
Lunar Phase (%): 48
Estimated In-Band Irradiance ($\mu W/cm^2$):

| Vehicle Sites Viewed | Approximate Line of Sight and Range | |
|---|---|---|
| VS5 (M-151 Jeep) | | 330 yds |
| VS6 (M-1 Tank) | 211° | 330 yds |
| VS7 (Soviet ZIL) | | 330 yds |
| M-15 Anti-Tank Mines | | 10 yds |

Additional Comments

Line of sight toward VS6. Mines in foreground exhibit limited polarization. Scene still in twilight

Sky is fully overcast.

Scene 33

Date: 22 September 1989
Time: 0738 hrs
Sensor Used: Spectral filters alternating at 2.5 Hz in front of L3 scope. Output monitored using CCD camera.

Observation Point: OP1 (Dredge/Fill Site)
Sun Elevation (deg): 8.9 Azimuth: 95.5
Moon Elevation (deg): 82.5 Azimuth: 228.3
Lunar Phase (%): 48
Estimated In-Band Irradiance ($\mu W/cm^2$):

| Vehicle Sites Viewed | | Approximate Line of Sight and Range |
|---|---|---|
| VS5 (M-151 Jeep) | | 330 yds |
| VS6 (M-1 Tank) | 211° | 330 yds |
| VS7 (Soviet ZIL) | | 330 yds |

Additional Comments

Line of sight toward VS6. Vehicles exhibit significant modulation. Moderate ground fog. Filter transmissions balanced for vegetation.

Sky is fully overcast.

Scene 34

Date: 22 September 1989
Time: 0746 hrs
Sensor Used: Spectral filters alternating at 2.5 Hz in front of L3 scope. Output monitored using CCD camera.

Observation Point: OP3 (Dredge/Fill Site)
Sun Elevation (deg): 10.6 Azimuth: 96.6
Moon Elevation (deg): 81.2 Azimuth: 236.3
Lunar Phase (%): 48
Estimated In-Band Irradiance ($\mu W/cm^2$):

| Vehicle Sites Viewed | Line of Sight (approximate) | |
|---|---|---|
| VS4 (M-113 APC) | 206° | 90 yds |
| VS5 (M-151 Jeep) | 191° | 80 yds |
| VS6 (M-1 Tank) | 181° | 80 yds |
| VS7 (Soviet ZIL) | 171° | 100 yds |

Additional Comments

Line of sight on VS6. Image pans to jeep then to M-113. Strong modulation from the M-1 and the ZIL. Jeep and M-113 also modulate.

Sensor blooming caused by sky falling within the field of view causes difficulties in viewing Jeep and M-113.

Sky is fully overcast.

Scene 35

Date: 22 September 1989
Time: 0950 hrs
Sensor Used: Spectral filters alternating at 2.5 Hz in front of L3 scope. Output monitored using CCD camera.

Observation Point: OP7 (Poor House Site)
Sun Elevation (deg): 35.6 Azimuth: 116.7
Moon Elevation (deg): 56.4 Azimuth: 271.1
Lunar Phase (%): 48
Estimated In-Band Irradiance (W/cm^2):

| Vehicle Sites Viewed | Approximate Line of Sight and Range | |
|---|---|---|
| VS12 (M-2 Bradley) | 66° | 150 yds |

Additional Comments

Line of sight toward VS12. Target appears to modulate, however, sensor blooming makes image difficult to view.

Sky is fully overcast.

Scene 36

Date: 22 September 1989
Time: 1012 hrs
Sensor Used: Spectral filters alternating at 2.5 Hz in front of L3 scope. Output monitored using CCD camera.

Observation Point: OP1 (Dredge/Fill Site)
Sun Elevation (deg): 39.6 Azimuth: 121.4
Moon Elevation (deg): 51.9 Azimuth: 273.6
Lunar Phase (%): 48
Estimated In-Band Irradiance (W/cm^2):

| Vehicle Sites Viewed | Approximate Line of Sight and Range | |
|---|---|---|
| VS3 (M-60 Tank) | | 360 yds |
| VS4 (M-113 APC) | | 340 yds |
| VS5 (M-151 Jeep) | | 330 yds |
| VS6 (M-1 Tank) | 211° | 330 yds |
| VS7 (Soviet ZIL) | | 330 yds |

Additional Comments

Line of sight on VS6. Targets are modulating and road (gravel) is modulating. Sky within field of view causes sensor blooming.

Sky is fully overcast.

Scene 37

Date: 22 September 1989
Time: 1013 hrs
Sensor Used: Spectral filters alternating at 2.5 Hz in front of L3 scope. Output monitored using CCD camera.

Observation Point: OP1 (Dredge/Fill Site)
Sun Elevation (deg): 39.8 Azimuth: 121.7
Moon Elevation (deg): 51.7 Azimuth: 273.7
Lunar Phase (%): 48
Estimated In-Band Irradiance (W/cm^2):

| Vehicle Sites Viewed | Approximate Line of Sight and Range |
|---|---|
| M-15 Anti Tank Mines | About 15 feet |

Additional Comments

Close up of a M-15 mine. Mine and bare soil modulating. Sky is fully overcast.

Scene 38

Date: 22 September 1989
Time: 1042 hrs
Sensor Used: Spectral filters alternating at 2.5 Hz in front of L3 scope. Output monitored using CCD camera.

Observation Point: OP3 (Dredge/Fill Site)
Sun Elevation (deg): 44.8 Azimuth: 128.8
Moon Elevation (deg): 45.7 Azimuth: 276.8
Lunar Phase (%): 48
Estimated In-Band Irradiance (W/cm^2):

| Vehicle Sites Viewed | Approximate Line of Sight and Range | |
|---|---|---|
| VS3 (M-60 Tank) | 218° | 110 yds |
| VS4 (M-113 APC) | 206° | 90 yds |
| VS5 (M-151 Jeep) | 191° | 80 yds |
| VS6 (M-1 Tank) | 181° | 80 yds |
| VS7 (Soviet ZIL) | 171° | 100 yds |

Additional Comments

Line of sight on VS6. Image then pans to VS5, to VS4 and VS3 and then back to VS6. Sensor is then zoomed and refocused. All vehicles exhibit significant modulation. The M-1 has a camouflage net draped over the barrel and the front end of the turret. Net exhibits some modulation.

Sky is fully overcast.

Scene 39

Date: 22 September 1989
Time: 1053 hrs
Sensor Used: Dichroic polarizer cycling at 2.5 Hz in front of CCD camera.

Observation Point: OP3 (Dredge/Fill Site)
Sun Elevation (deg): 46.6 Azimuth: 131.8
Moon Elevation (deg): 43.5 Azimuth: 277.9
Lunar Phase (%): 48
Estimated In-Band Irradiance (W/cm^2):

| Vehicle Sites Viewed | Approximate Line of Sight and Range | |
|---|---|---|
| VS6 (M-1 Tank) | 181° | 80 yds |
| VS7 (Soviet ZIL) | 171° | 100 yds |

Additional Comments

Line of sight is on VS6. The M-1 has a camouflage net draped over the barrel and the front end of the turret. The M-1 exhibits strong polarization on some facets. Some polarization can be seen on net and on facets visible through net.

Sky is fully overcast.

## Appendix B. SOLAR AND LUNAR COORDINATES

The following tables give the elevation and azimuth of the sun and moon during the data collection session. Times are given in local Central Daylight Time and the coordinates are the coordinates for the centroid of each astronomical body. The phase of the moon is the percent of the total moon surface viewable from earth that is illuminated by the sun. Rise and set times are the times at which the centroid of each body crosses the astronomical horizon.

Date: 18 September 1989

Sun Rise: 0600 hrs  Moon Set: 1000 hrs
Sun Set: 1900 hrs  Moon Rise: 2100 hrs

| Time | Sun Elevation | Sun Azimuth | Moon Elevation | Moon Azimuth | Moon Phase(%) |
|---|---|---|---|---|---|
| 0000 | | | 42.8 | 101.6 | 80.1 |
| 0100 | | | 54.8 | 113.3 | 79.9 |
| 0200 | | | 65.4 | 132.5 | 79.7 |
| 0300 | | | 72.0 | 168.1 | 79.5 |
| 0400 | | | 70.0 | 212.3 | 79.3 |
| 0500 | | | 61.1 | 239.7 | 79.1 |
| 0600 | | | 49.8 | 254.9 | 78.8 |
| 0700 | 1.4 | 88.8 | 37.8 | 265.0 | 78.6 |
| 0800 | 14.0 | 97.0 | 25.6 | 273.2 | 78.3 |
| 0900 | 26.4 | 106.0 | 13.6 | 280.6 | 78.1 |
| 1000 | 38.2 | 117.0 | 1.8 | 288.2 | 77.7 |
| 1100 | 48.7 | 132.0 | | | 77.4 |
| 1200 | 56.4 | 153.3 | | | 77.0 |
| 1300 | 59.3 | 181.1 | | | 76.7 |
| 1400 | 55.9 | 208.7 | | | 76.2 |
| 1500 | 47.9 | 229.3 | | | 75.8 |
| 1600 | 37.3 | 243.8 | | | 75.4 |
| 1700 | 25.4 | 254.6 | | | 75.0 |
| 1800 | 13.0 | 263.5 | | | 74.5 |
| 1900 | 0.3 | 271.7 | | | 74.1 |
| 2000 | | | | | 73.7 |
| 2100 | | | | | 73.4 |
| 2200 | | | 10.1 | 73.6 | 73.0 |
| 2300 | | | 22.2 | 80.3 | 72.7 |

Date: 19 September 1989

Sun Rise: 0654 hrs  Moon Set: 1123 hrs
Sun Set: 1901 hrs  Moon Rise: 2151 hrs

| Time | Sun Elevation | Sun Azimuth | Moon Elevation | Moon Azimuth | Moon Phase(%) |
|---|---|---|---|---|---|
| 0000 | | | 34.5 | 87.1 | 72.4 |
| 0100 | | | 46.9 | 94.8 | 72.1 |
| 0200 | | | 59.2 | 105.1 | 71.9 |
| 0300 | | | 70.6 | 123.4 | 71.7 |
| 0400 | | | 78.2 | 168.4 | 71.5 |
| 0500 | | | 74.3 | 226.5 | 71.3 |
| 0600 | | | 63.7 | 251.5 | 71.1 |
| 0700 | 1.3 | 89.2 | 51.7 | 263.8 | 70.9 |
| 0800 | 13.9 | 97.4 | 39.5 | 272.3 | 70.6 |
| 0900 | 26.3 | 106.4 | 27.3 | 279.4 | 70.4 |
| 1000 | 38.0 | 117.5 | 15.5 | 286.2 | 70.1 |
| 1100 | 48.4 | 132.4 | 4.1 | 293.4 | 69.8 |
| 1200 | 56.1 | 153.7 | | | 69.4 |
| 1300 | 58.9 | 181.3 | | | 69.1 |
| 1400 | 55.5 | 208.5 | | | 68.7 |
| 1500 | 47.5 | 229.1 | | | 68.3 |
| 1600 | 37.0 | 243.5 | | | 67.9 |
| 1700 | 25.1 | 254.3 | | | 67.4 |
| 1800 | 12.7 | 263.2 | | | 67.0 |
| 1900 | 0.05 | 271.4 | | | 66.6 |
| 2000 | | | | | 66.2 |
| 2100 | | | | | 65.8 |
| 2200 | | | 1.7 | 62.7 | 65.4 |
| 2300 | | | 13.0 | 70.0 | 65.1 |

Date: 20 September 1989

Sun Rise: 0655 hrs  Moon Set: 1235 hrs
Sun Set: 1859 hrs  Moon Rise: 2242 hrs

| Time | Sun Elevation | Sun Azimuth | Moon Elevation | Moon Azimuth | Moon Phase(%) |
|---|---|---|---|---|---|
| 0000 | | | 24.7 | 75.9 | 64.7 |
| 0100 | | | 36.8 | 82.1 | 64.5 |
| 0200 | | | 49.1 | 88.7 | 64.2 |
| 0300 | | | 61.5 | 97.2 | 64.0 |
| 0400 | | | 73.5 | 112.2 | 63.8 |
| 0500 | | | 82.5 | 164.2 | 63.6 |
| 0600 | | | 77.1 | 240.0 | 63.4 |
| 0700 | 1.2 | 89.6 | 65.4 | 260.5 | 63.2 |
| 0800 | 13.8 | 97.8 | 53.2 | 270.2 | 62.9 |
| 0900 | 26.1 | 106.8 | 41.0 | 277.2 | 62.7 |
| 1000 | 37.8 | 117.9 | 28.9 | 283.5 | 62.5 |
| 1100 | 48.2 | 132.9 | 17.3 | 289.8 | 62.2 |
| 1200 | 55.8 | 154.1 | 6.1 | 296.6 | 61.9 |
| 1300 | 58.5 | 181.5 | | | 61.5 |
| 1400 | 55.2 | 208.4 | | | 61.2 |
| 1500 | 47.2 | 228.8 | | | 60.8 |
| 1600 | 36.6 | 243.2 | | | 60.4 |
| 1700 | 24.8 | 254.1 | | | 60.0 |
| 1800 | 12.4 | 263.0 | | | 59.5 |
| 1900 | | | | | 59.1 |
| 2000 | | | | | 58.7 |
| 2100 | | | | | 58.3 |
| 2200 | | | | | 57.9 |
| 2300 | | | 3.2 | 60.3 | 57.5 |

Date: 21 September 1989

Sun Rise: 0656 hrs  Moon Set: 1342 hrs
Sun Set: 1858 hrs  Moon Rise: 2342 hrs

| Time | Sun Elevation | Sun Azimuth | Moon Elevation | Moon Azimuth | Moon Phase(%) |
|---|---|---|---|---|---|
| 0000 | | | 14.1 | 67.1 | 57.2 |
| 0100 | | | 25.6 | 73.2 | 56.9 |
| 0200 | | | 37.5 | 79.0 | 56.6 |
| 0300 | | | 49.7 | 85.0 | 56.4 |
| 0400 | | | 62.0 | 92.2 | 56.2 |
| 0500 | | | 74.3 | 104.2 | 56.0 |
| 0600 | | | 84.5 | 154.8 | 55.8 |
| 0700 | 1.0 | 89.9 | 78.5 | 247.6 | 55.6 |
| 0800 | 13.6 | 98.1 | 66.5 | 264.8 | 55.4 |
| 0900 | 26.0 | 107.2 | 54.2 | 273.0 | 55.2 |
| 1000 | 37.6 | 118.4 | 42.0 | 279.3 | 54.9 |
| 1100 | 47.9 | 133.4 | 30.0 | 285.2 | 54.7 |
| 1200 | 55.4 | 154.5 | 18.4 | 291.1 | 54.4 |
| 1300 | 58.1 | 181.6 | 7.3 | 297.6 | 54.1 |
| 1400 | 54.8 | 208.3 | | | 53.8 |
| 1500 | 46.8 | 228.5 | | | 53.4 |
| 1600 | 36.3 | 243.0 | | | 53.0 |
| 1700 | 24.5 | 253.8 | | | 52.6 |
| 1800 | 12.1 | 262.7 | | | 52.2 |
| 1900 | | | | | 51.8 |
| 2000 | | | | | 51.4 |
| 2100 | | | | | 51.0 |
| 2200 | | | | | 50.6 |
| 2300 | | | | | 50.2 |

Date: 22 September 1989

Sun Rise: 0656 hrs  Moon Set: 1440 hrs
Sun Set: 1857 hrs

| Time | Sun Elevation | Sun Azimuth | Moon Elevation | Moon Azimuth | Moon Phase(%) |
|---|---|---|---|---|---|
| 0000 | | | 3.1 | 59.6 | 49.8 |
| 0100 | | | 14.0 | 66.5 | 49.5 |
| 0200 | | | 25.4 | 72.6 | 49.2 |
| 0300 | | | 37.3 | 78.5 | 49.0 |
| 0400 | | | 49.4 | 84.6 | 48.7 |
| 0500 | | | 61.7 | 91.8 | 48.5 |
| 0600 | | | 73.9 | 103.8 | 48.3 |
| 0700 | 0.9 | 90.3 | 84.3 | 152.2 | 48.1 |
| 0800 | 13.5 | 98.5 | 78.7 | 245.9 | 48.0 |
| 0900 | 25.8 | 107.6 | 66.7 | 263.9 | 47.8 |
| 1000 | 37.5 | 118.8 | 54.3 | 272.3 | 47.6 |
| 1100 | 47.7 | 133.8 | 42.1 | 278.6 | 47.3 |
| 1200 | 55.1 | 154.9 | 30.0 | 284.4 | 47.1 |
| 1300 | 57.7 | 181.8 | 18.3 | 290.4 | 46.8 |
| 1400 | 54.4 | 208.1 | 7.1 | 296.9 | 46.5 |
| 1500 | 46.5 | 228.3 | | | 46.2 |
| 1600 | 36.0 | 242.7 | | | 45.8 |
| 1700 | 24.2 | 253.5 | | | 45.4 |
| 1800 | 11.8 | 262.4 | | | 45.0 |
| 1900 | | | | | 44.6 |
| 2000 | | | | | 44.2 |
| 2100 | | | | | 43.8 |
| 2200 | | | | | 43.4 |
| 2300 | | | | | 43.0 |

# APPENDIX C. IMAGES ANALYZED

The photographs presented here are photographs of the images that were analyzed quantitatively along with corresponding daylight color photographs of the same scene. They are presented here as an aid to the reader in forming conclusions as to target detectability.

89-12021-5

Figure C-1a. M-113, Scene 5, Conventional Image

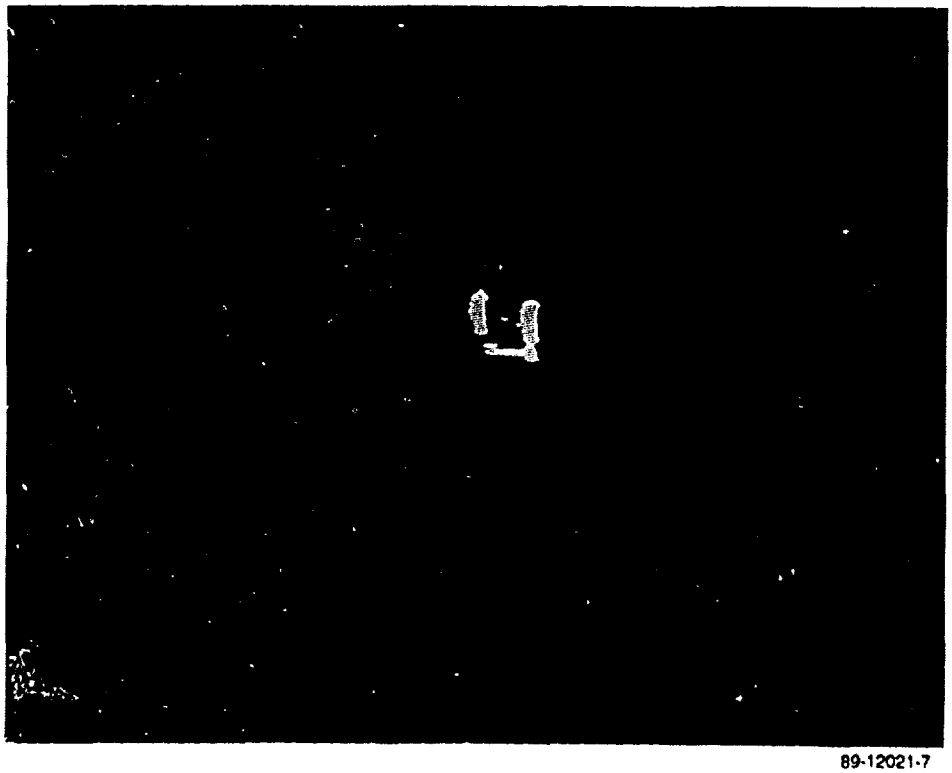

89-12021-7

Figure C-1b. M-113, Scene 5, Modulation Image (Polar)

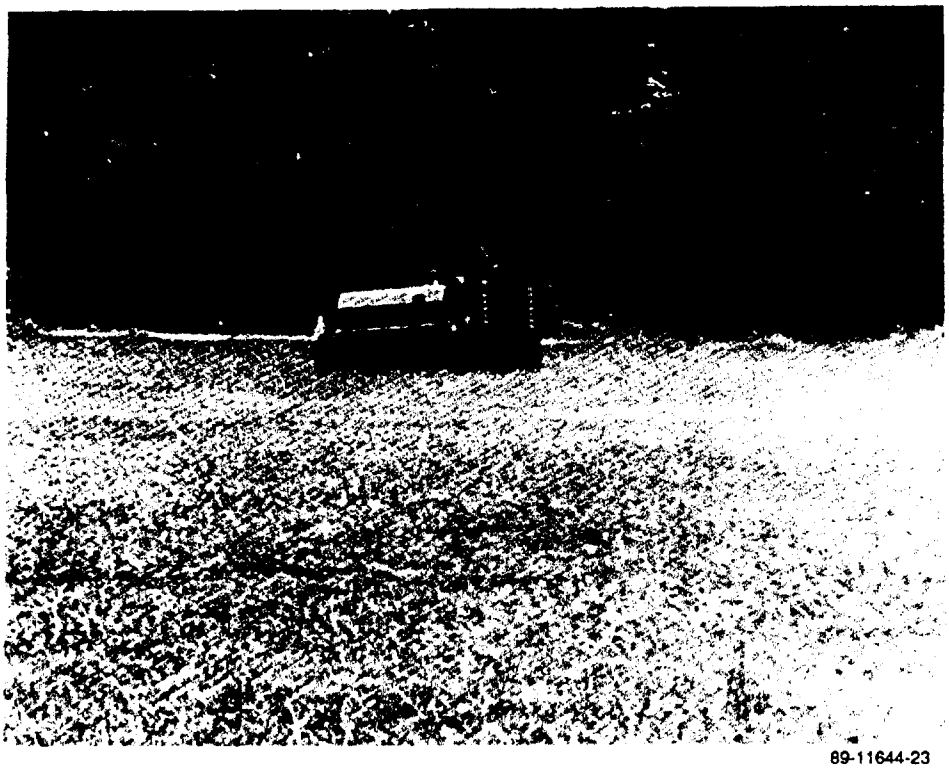

89-11644-23

Figure C-1c. M-113, Daylight Photograph (Scene 5)

89-12021-2

Figure C-2a. M-113, Scene 3, Conventional Image

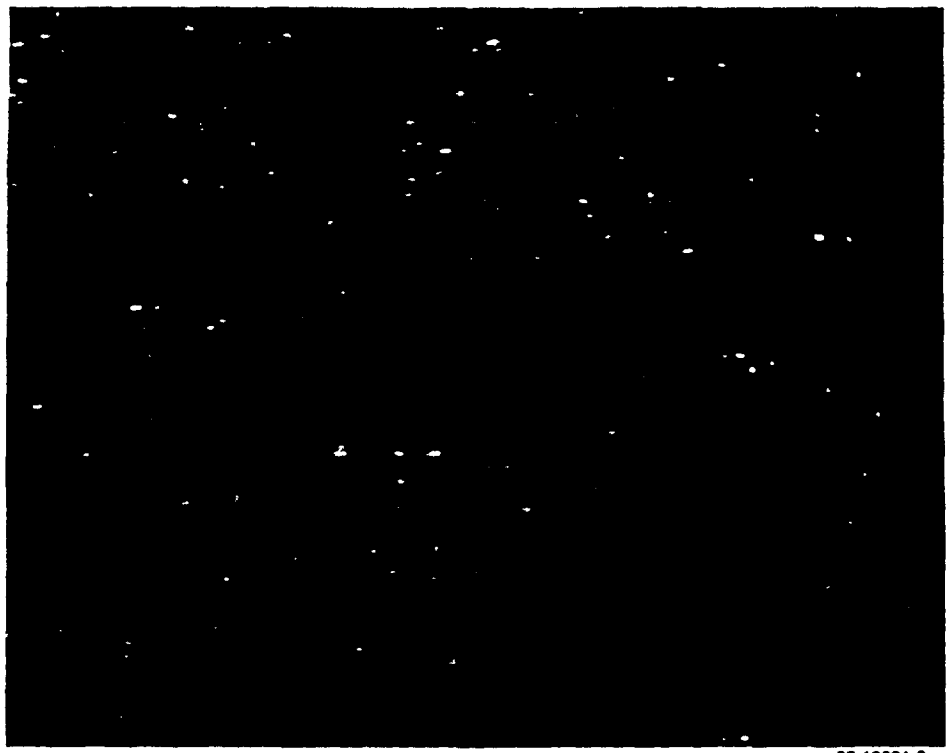

89-12021-3

Figure C-2b. M-113, Scene 3, Modulation Image (Polar)

89-11644-9

Figure C-2c. M-113, Daylight Photograph (Scene 3)

89-12022-14

Figure C-3a. Automobile, Scene 16, Conventional Image

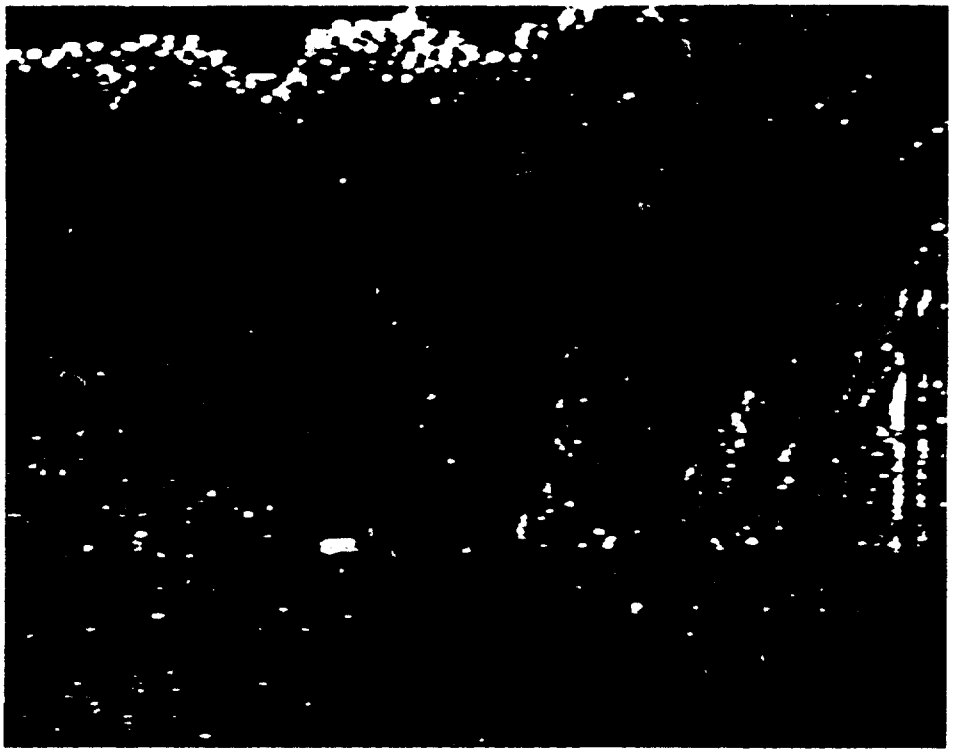

89-12022-16

Figure C-3b. Automobile, Scene 16, Modulation Image (Polar)

89-11645-8

Figure C-3c. Automobile, Daylight Photograph (Scene 16)

89-12021-10

Figure C-4a. M-113, Scene 9, Conventional Image

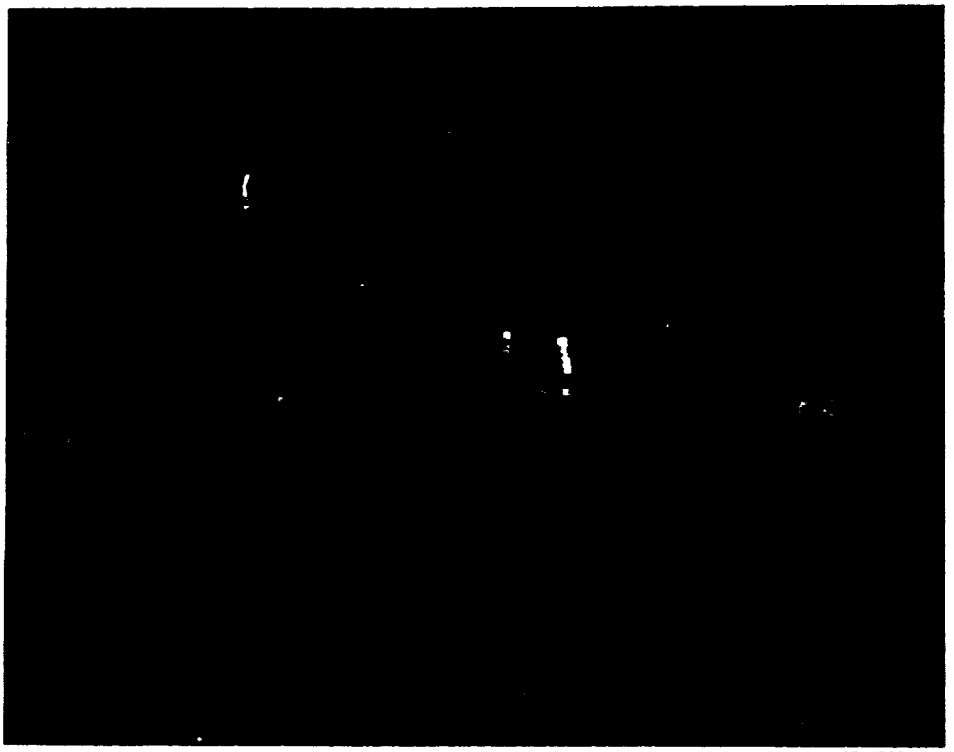

89-12021-11

Figure C-4b. M-113, Scene 9, Modulation Image (Polar)

89-11644-23

Figure C-4c. M-113, Daylight Photograph

**Preceding Page Blank**

89-12021-14

Figure C-5a Jeep, Scene 9, Conventional Image

89-12021-15

Figure C-5b. Jeep, Scene 9, Modulation Image (Polar)

89-11644-23

Figure C-5c. Jeep, Daylight Photograph (Scene 9)

89-12021-19

Figure C-6a. ZIL, Scene 9, Conventional Image

89-12021-21

Figure C-6b. ZIL, Scene 9, Modulation Image (Polar)

89-11644-23

Figure C-6c. ZIL, Daylight Photograph (Scene 9)

89-12021-24

Figure C-7a. M-113, Scene 13, Conventional Image

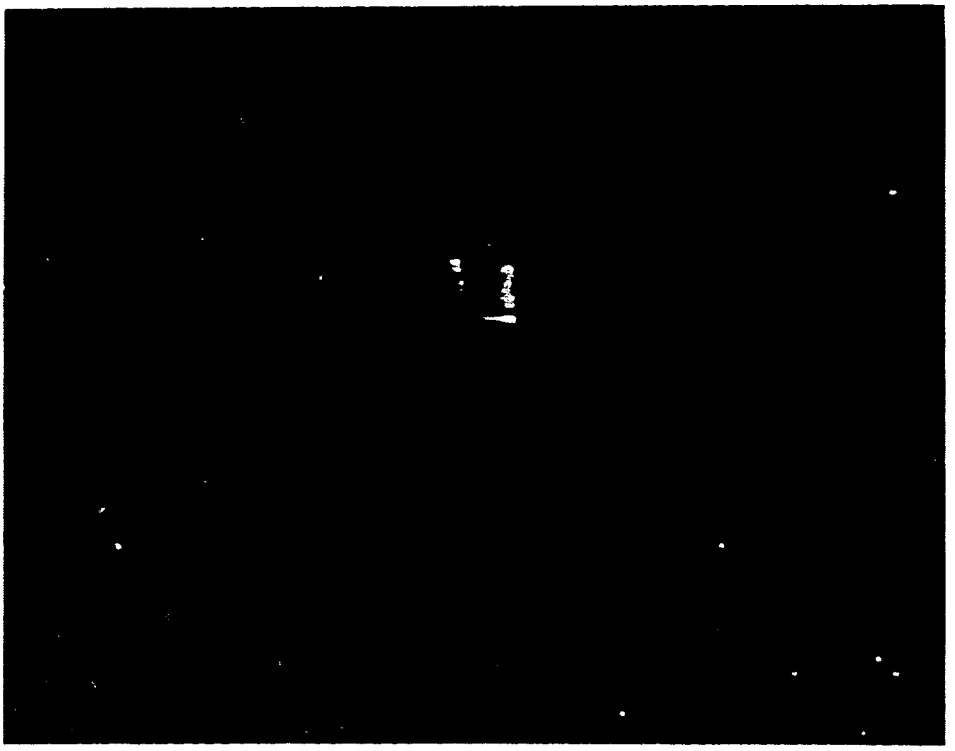

89-12021-25

Figure C-7b. M-113, Scene 13, Modulation Image (White Stripes)

89-12021-27

Figure C-7c. M-113, Scene 13, Modulation Image (O.D. Paint)

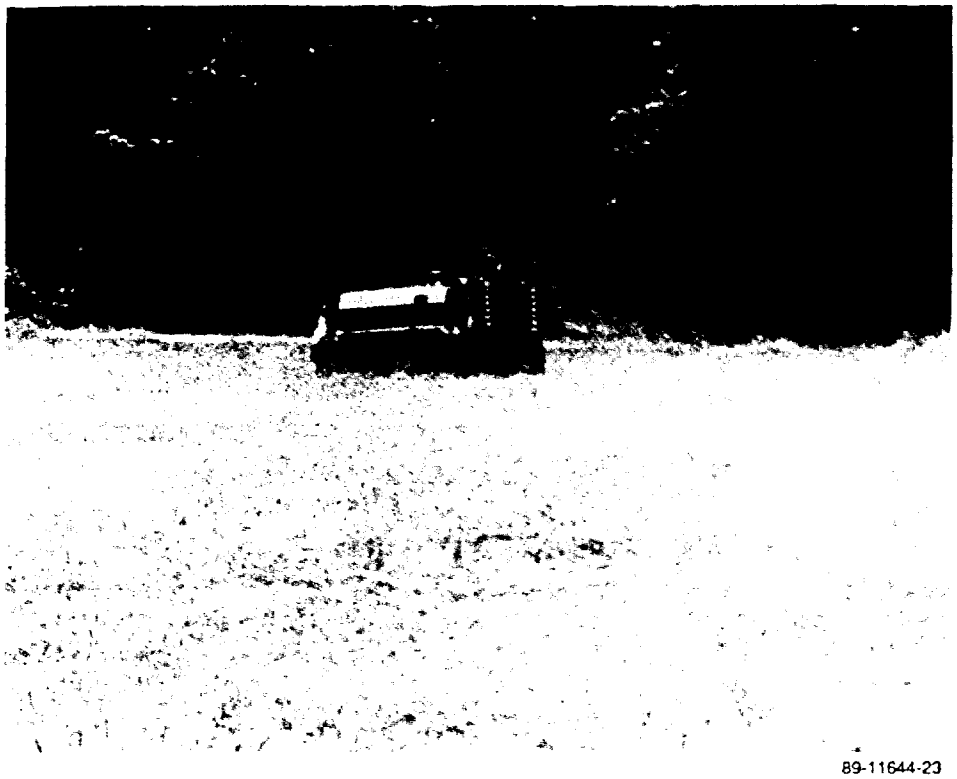

89-11644-23

Figure C-7d. M-113, Daylight Photograph

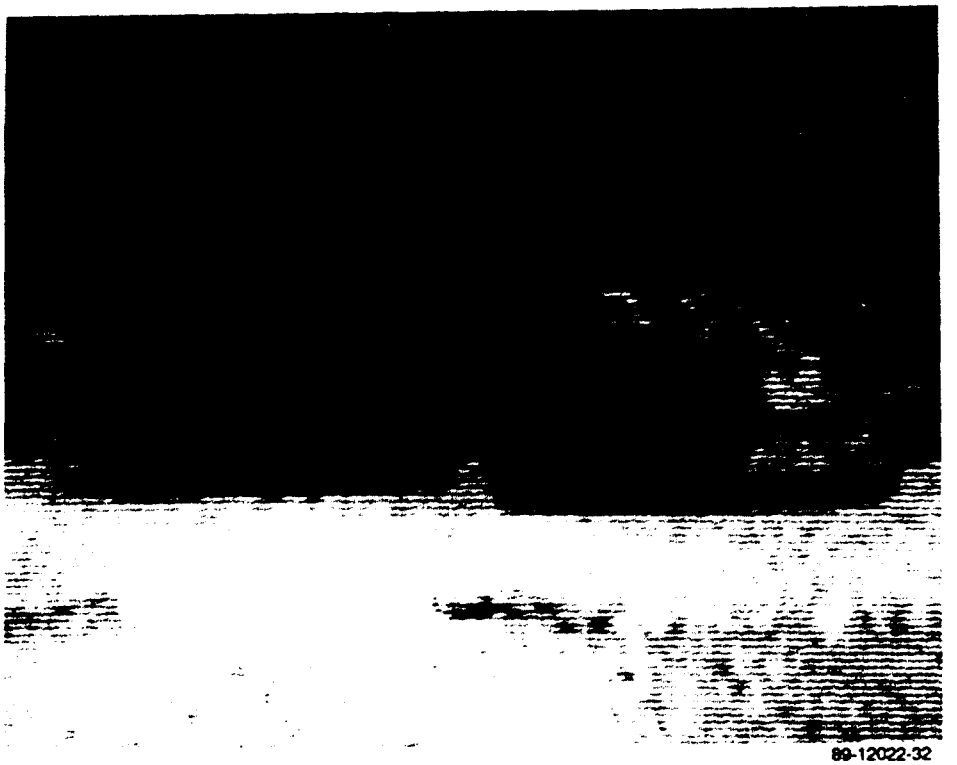


Figure C-8a. M-1 and ZIL, Scene 25, Conventional Image


Figure C-8b. M-1 and ZIL, Scene 25, Modulation Image (Polar)

89-12022-18

Figure C-9a. M-1 and ZIL, Scene 39, Conventional Image

89-12022-20

Figure C-9b. M-1 and ZIL, Scene 39, Modulation Image (Polar)

89-11645-18

Figure C-9c. M-1 and ZIL, Daylight Photograph (Scene 39)

89-12022-22

Figure C-10a. M-2, Scene 15, Conventional Image

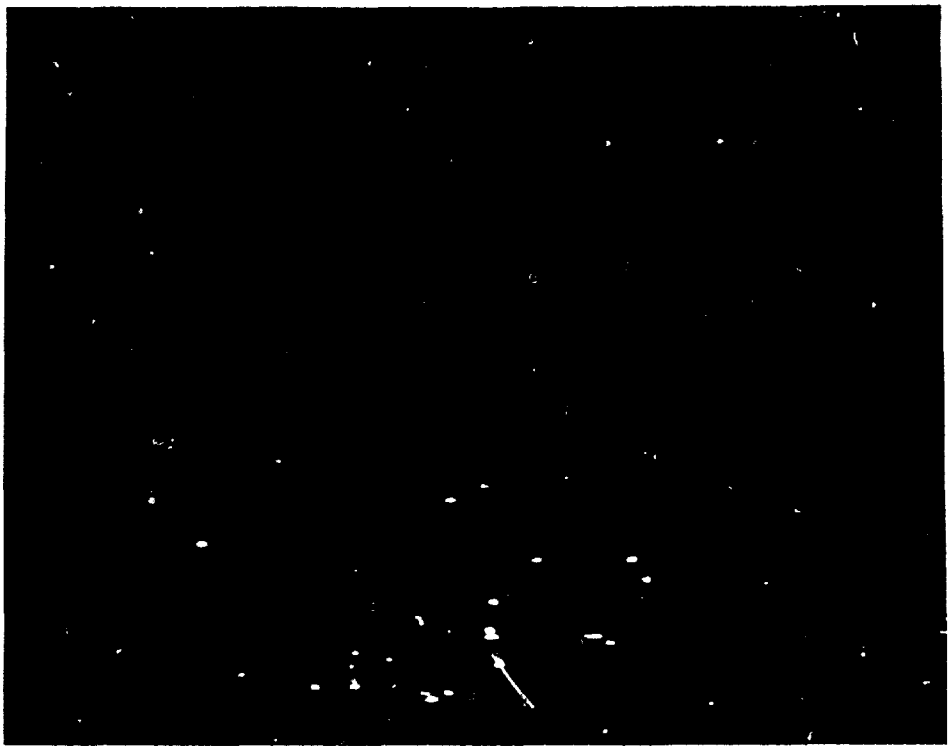

89-12022-24

Figure C-10b. M-2, Scene 15, Modulation Image (Polar)

89-11643-11

Figure C-10c. M-2, Daylight Photograph (Scene 15)

89-12023-3A

Figure C-11a. M-1 and ZIL, Scene 20, Conventional Image

89-12023-4A

Figure C-11b. M-1 and ZIL, Scene 20, Modulation Image (Polar)

89-11645-11

Figure C-11c. M-1 and ZIL, Daylight Photograph (Scene 20)

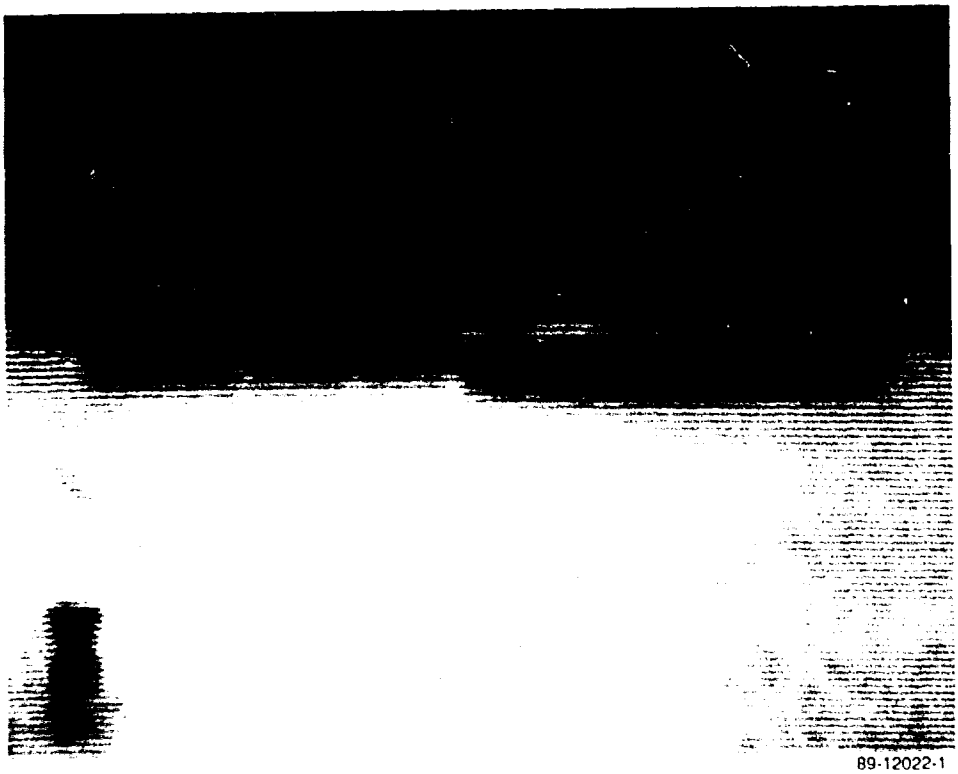

89-12022-1

Figure C-12a. M-1 and ZIL, Scene 34, Image Average

89-12022-2

Figure C-12b. M-1 and ZIL, Scene 34, Modulation Image (Spectral)

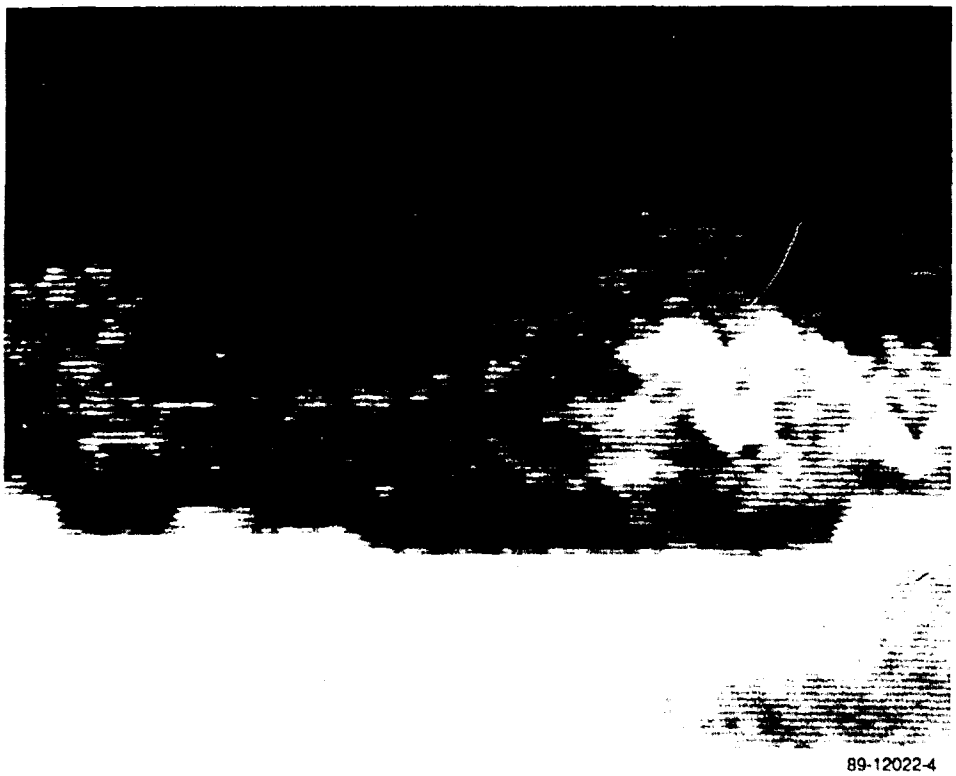

89-12022-4

Figure C-13a. M-1 and ZIL, Scene 38, Image Average

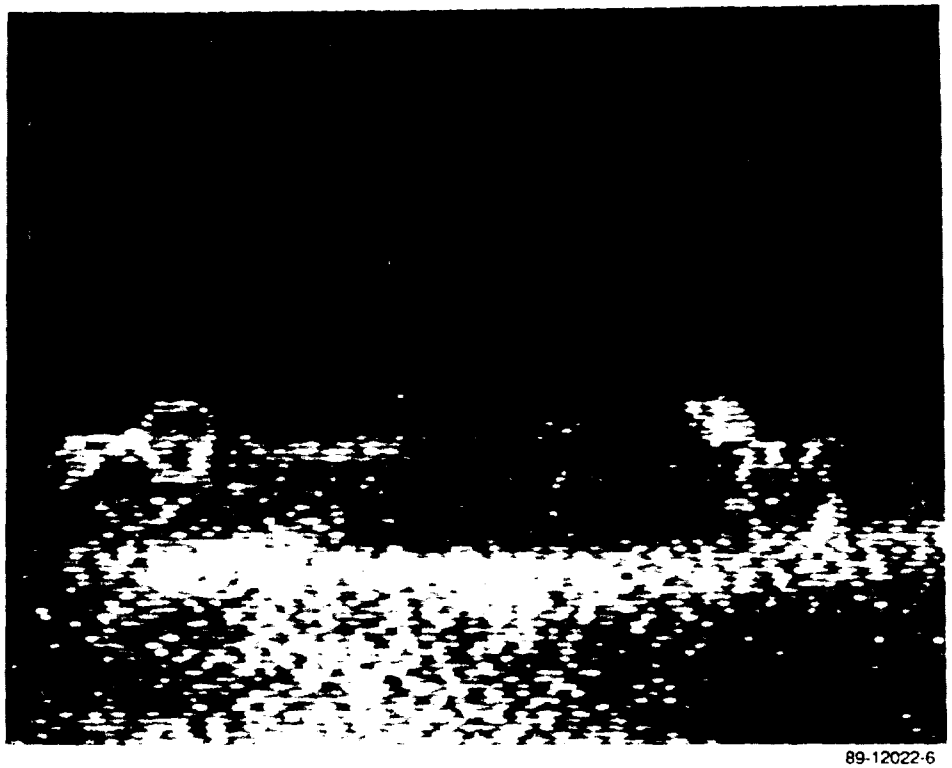

89-12022-6

Figure C-13b. M-1 and ZIL, Scene 38, Modulation Image (Spectral)

89-11645-18

Figure C-13c. M-1 and ZIL, Daylight Photograph (Note Camouflage Net)



**Preceding Page Blank**

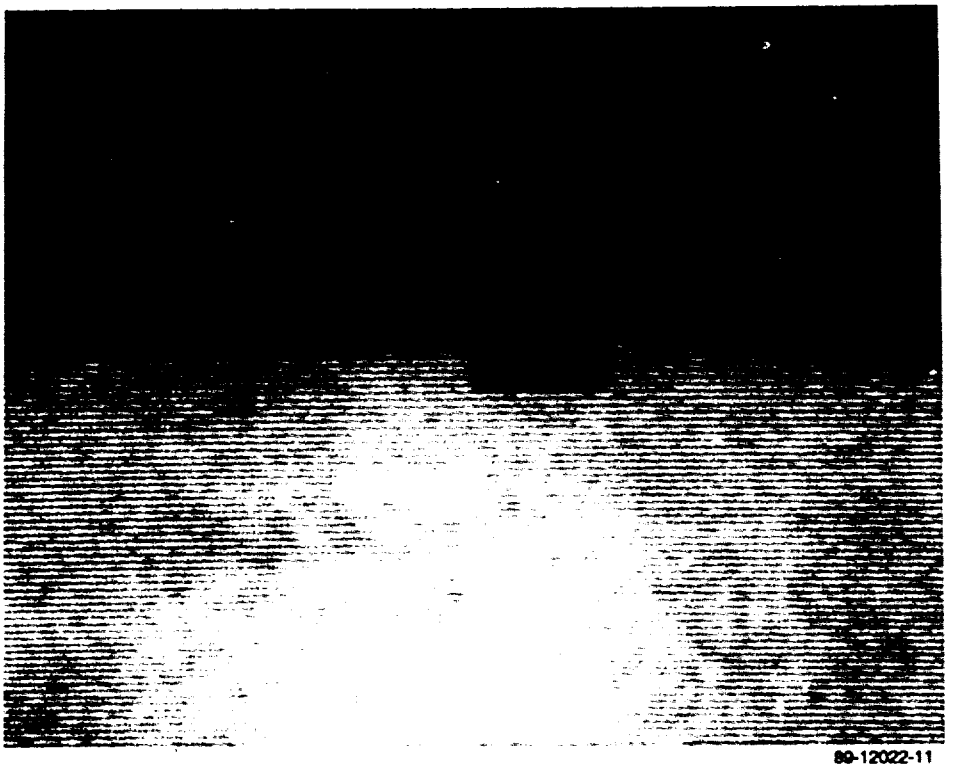

89-12022-11

Figure C-14a. Jeep, Scene 34, Image Average

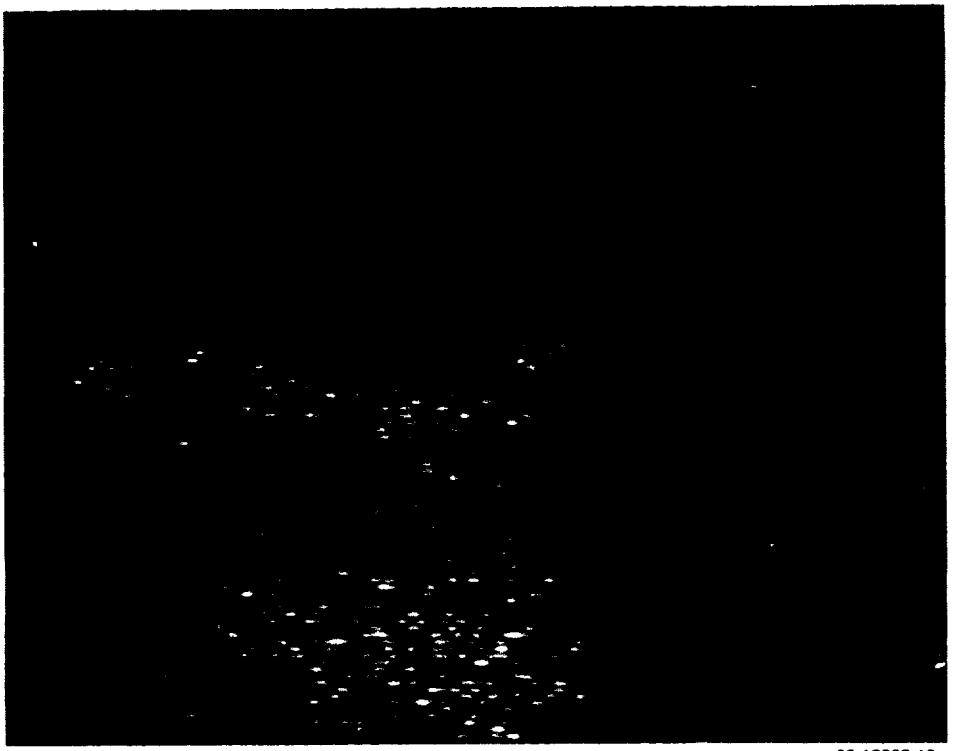

89-12022-12

Figure C-14b. Jeep, Scene 34, Modulation Image (Spectral)

**Preceding Page Blank**


Figure C-14c. Jeep, Daylight Photograph (Scene 34)


Figure C-15a. ZIL, Scene 1, Conventional Image

Preceding Page Blank

89-12022-28

Figure C-15b. ZIL, Scene 1, Modulation Image (Spectral)

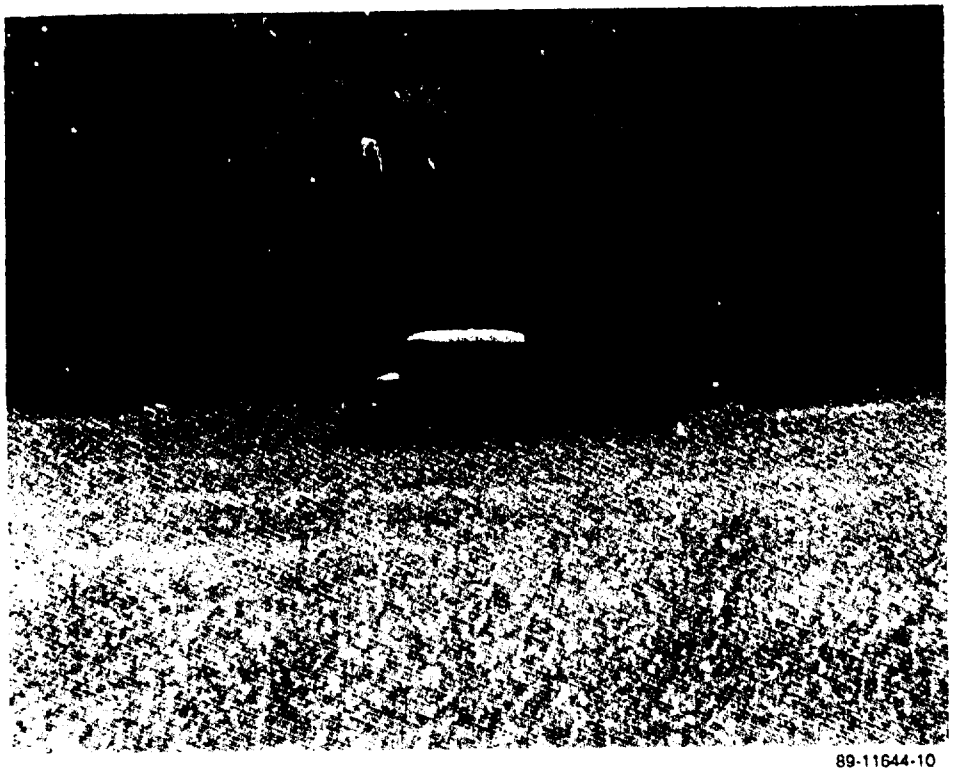

89-11644-10

Figure C-15c. ZIL, Daylight Photograph (Scene 1)

Preceding Page Blank

89-12022-35

Figure C-16a. M-113 and M-60, Scene 34, Image Average

89-12023-0A

Figure C-16b. M-113 and M-60, Scene 34, Modulation Image (Spectral)


Figure C-16c. M-113 and M-60, Daylight Photograph (Scene 34)

Preceding Page Blank

DISTRIBUTION LIST

US Army LABCOM (2 copies)
ATTN: AMSLC-TP (Dr. Gonano)
2800 Powder Mill Road
Adelphi, MD 20783-1197

Commander (2 copies)
US Army Corps of Engineers
ATTN: CERD-M (J. Lundien)
20 Massachusetts Avenue NW
Washington, DC 20314

Commander
US Army Combined Arms Combat
Development Activity
ATTN: ATZL-CA
Fort Leavenworth, KS 66027-5320

Commander
US Army Belvoir Research,
Development, and Engineering
Center
ATTN: STRBE-N
Fort Belvoir, VA 22060-5606

Commander
US Army Intelligence Center and
School
ATTN: ATSI-CD
Fort Huachuca, AZ 85613-7000

Commander
US Army Research Office
ATTN: Dr. Steve J. Mock
PO Box 12211
Research Triangle Park, NC 27709

Director
US Army Countermeasure/Counter-
Countermeasure Center
ATTN: DRXCM-EO
2800 Powder Mill Road
Adelphi, MD 20783

Commander
USAE Waterways Experiment
Station (5 copies)
ATTN: WESEN-B
P.O. Box 631
Vicksburg, MS 39180-0631

Commander
US Army Training and Doctrine
Command
ATTN: ATTG-A
Fort Monroe, VA 23651

Commander
US Army Infantry School
ATTN: ATZQ-D-MS
Fort Benning, GA 31905

Commander
US Army Military Police and
Chemical Schools/Training
Center
ATTN: ATZN-MP-CD
Fort McClellan, AL 36205

Commander
US Marine Corps Development and
Education Command
Quantico, VA 22134

Commander
US Army Combat Surveillance and
Target Acquisition
Laboratory
ATTN: DELCS-R/Mr. Vandeermeer
Fort Monmouth, NJ 07703

US Army Deputy Chief of Staff
for Research, Development,
and Acquisition
ATTN: DAMA-ARZ-A
The Pentagon
Washington, DC 20310

Director (2 copies)
Defense Technical Information Center
ATTN: DDAB
Cameron Station
Alexandria, VA 22314

Office of the Under Secretary of Defense for Research and Engineering
The Pentagon, Room 3D129
Washington, DC 20310

Commander
US Army Armament Research, Development, and Engineering Center
ATTN: SMCAR-ASM
Picatinny Arsenal, NJ 07806-5000

Director
Center for Night Vision and Electro-Optics
ATTN: AMSEL-RO-NV-SP (Miller)
Fort Belvoir, VA 22060-5677

Headquarters
Department of the Army
ATTN: DAEN
The Pentagon, Room 1E676
Washington, DC 20310-2600

Commander
US Army Test and Evaluation Command
ATTN: DRSTE-RU
Aberdeen Proving Ground, MD 21005

Commander
US Army TRADOC Analysis Command
ATTN: ATRC-WSR
White Sands Missile Range, NM 88002-5502